ASCMO

Open Access

Supplement of

Evaluation of simulated responses to climate forcings: a flexible statistical framework using confirmatory factor analysis and structural equation modelling – Part 2: Numerical experiment

Katarina Lashgari et al.

Correspondence to: Katarina Lashgari (katarina.lashgari@gmail.com)

Contents

35

40

45

50

S1 Interpretation of the numerical results

This section complements Sect. 4 in Lashgari et al. (2022) (henceforth referred to as LAS22num) by providing details and discussions of the numerical results for the Europe, Arctic, Asia, South America, Australasia and Antarctica regions. All subsections have the same structure, namely:

1. The presentation of the data sets analysed.

   As motivated in Sect. 2 in LAS22num, some ensembles have been reduced by eliminating some of their members. Therefore, we first present the remaining members of each ensemble, used to construct corresponding mean sequences.

2. The presentation of the preliminary analyses of the final single-forcing ensembles.

   To get a preliminary idea about the magnitude of the effect of forcing f on the simulated temperature in each region, each final ensemble is also analysed by means of the CFA(k_f, 1) model, where k_f is the number of the remaining ensemble members, and $f \in \{$Sol, Orb, Volc, Land (anthr), GHG, comb$\}$. The CFA(k_f, 1) model is defined in Sect. 2.1 in Eq. (4). Here, the main model parameter of interest is the factor loading α_f, representing the effect of forcing f on the temperature. The resulting estimates of each α_f is then used for assessing the reliability and appropriateness of the estimates provided by the three statistical models of interest.

3. The presentation and interpretation of the numerical results for each of the three statistical models of interest.

   The statistical models, defined in LAS22num in Sect.3, are:

   (a) the ME-CFA(6, 5) model from Table 3 in LAS22num, which is a ME model rewritten in the form of a CFA model,

   (b) the CFA(7, 6) model from Table 5 in LAS22num, and

   (c) the SEM model whose path diagram is depicted in Fig. 1 in LAS22num.

Prior to presenting the numerical results, let us emphasize that the main concepts and definitions of a general SEM model, including a general CFA model as a special case, are given here in Sect. S2. Since CFA and SEM models are closely related, the way of assessing their overall fit to the data and determining their acceptability is the same (for the details see Sect. S2.4). As follows from Sect. S2.4, the model overall fit is to be judged both statistically by means of the χ^2 statistic, given in Eq. (S18), and heuristically by means of the goodness-of-fit indices GFI, AGFI and SRMR, given in Eq. (S19), (S20), and (S21), respectively.

It is also worth emphasising that in our statistical analyses we have used the 5% significance level for making inferences concerning various hypotheses.

S1.1 Europe (summer, June-August, mean temperature)

80   The data sets analysed are presented in Table S1.1.1, from which it follows that seven data sets were analysed. Results for the three statistical models of interest are provided in Tables S1.1.2 - S1.1.4.

Table S1.1.1. Overview of replicates of each x_f, used to construct seven regional Europe data sets. Each data set contains different $\bar{x}_{\text{comb}}$ and τ_{pseudo}, where $\bar{x}_{\text{comb}}$ is constructed by averaging over three replicates randomly selected from the six that remained after $x_{\text{comb repl.}i}$:s, $i = 1, 6, 8$, have been eliminated and after one of $x_{\text{comb repl.}i}$:s, $i = 2, 3, 4, 5, 7, 9, 10$, is chosen to represent τ, i.e. τ_{pseudo}.

	Mean sequences					
Data set	x_{Sol}	x_{Orb}	x_{Volc}	$x_{\text{Land (anthr)}}, x_{\text{GHG}}$	x_{comb}	$x_{\text{comb repl.}i} = \tau_{\text{pseudo}}$
1	1,3	1,2	1,2,3,4	all associated repl's	4, 7, 10	2
2	1,3	1,2	1,2,3,4	all associated repl's	4, 5, 10	3
3	1,3	1,2	1,2,3,4	all associated repl's	2, 7, 9	4
4	1,3	1,2	1,2,3,4	all associated repl's	2, 3, 7	5
5	1,3	1,2	1,2,3,4	all associated repl's	2, 3, 9	7
6	1,3	1,2	1,2,3,4	all associated repl's	3, 5, 10	9
7	1,3	1,2	1,2,3,4	all associated repl's	3, 5, 7	10

S1.1.1 Preliminary analyses of final single-forcing ensembles by means of the CFA(k_f, 1) model

The analyses of the x_{Orb}-, and x_{Orb} ensembles, described in Table S1.1.1, indicated that the direct effect of the orbital respective land use forcing is not detected in the simulated summer mean temperature in Europe during $850-1849$ AD ($\widehat{\alpha}_{\text{Orb}} = 0.028$

85   with the associated p value of 0.50, $\widehat{\alpha}_{\text{Land (anthr)}} = 0.028$ with the associated p value of 0.31). In contrast, the similar analyses of x_{Sol}-, x_{Volc}-, and x_{GHG} ensembles suggested that the (direct) effects of the solar, volcanic respective GHG forcing are well pronounced in the simulated summer mean temperature in Europe during $850-1849$ AD ($\widehat{\alpha}_{\text{Sol}} = 0.063$ with p value$= 2.1e{-}04$, $\widehat{\alpha}_{\text{Volc}} = 0.134$ with p value$= 5.7e{-}26$, and $\widehat{\alpha}_{\text{GHG}} = 0.052$ with p value$= 0.001$).

S1.1.2 The result of fitting the ME-CFA(6, 5) model to the Europe data

90   Knowing that *Osim* and *Lsim* may be arbitrarily near zero, it is reasonable to expect various consequences of empirical under-identifiability, when fitting the ME-CFA(6, 5) model to the Europe data. As one can see in Table S1.1.2, the results confirm our apprehension. For those data sets, for which the estimation procedure has converged to a solution, the solutions obtained are inadmissble. This is reflected by inadmissble values of some correlation coefficients, which exceed 1 in absolut value. For example, for data set no. 1, it was observed $\widehat{\phi}_{OL} = 5.99$ and $\widehat{\phi}_{OG} = 1.14$.

95   Thus, the ME-CFA(6, 5) model has to be rejected for all data sets, despite its excellent fit to the data. For example, for data set no. 1, the p value for the χ^2 statistic, 0.57, is much larger than 0.05, and the observed values of the heuristic indices are within their acceptance areas: GFI $= 1 > 0.9$, AGFI $= 0.98 > 0.80$, and finally SRMR $= 0.008 < 0.08$.

Table S1.1.2. The result of estimating the ME-CFA(6, 5) model fitted to the Europe data. The estimates marked in bold font are inadmissble.

• *The result for data set no. 1*

Parameter	Estimate	p value	Parameter	Estimate	p value	Parameter	Estimate	p value
Ssim	0.064	4.7e–06	Lsim	0.029	0.19	ϕ_{SL}	-0.38	0.54
Strue	0.000	0.99	Ltrue	0.010	0.78	ϕ_{SG}	0.55	0.11
Osim	0.013	0.84	Gsim	0.051	2.7e–04	ϕ_{OV}	0.70	0.85
Otrue	0.004	0.87	Gtrue	0.032	0.72	ϕ_{OL}	**5.99**	0.84
Vsim	0.134	1.5e–26	ϕ_{SO}	0.16	0.92	ϕ_{OG}	**1.14**	0.85
Vtrue	0.130	5.3e–04	ϕ_{SV}	-0.03	0.86	ϕ_{VL}	0.86	0.18
			ϕ_{VG}	0.13	0.56	ϕ_{LG}	0.49	0.49

To assess the overall model fit:

$$\text{Model } \chi^2 = 0.315, \quad \text{df} = 1, \quad p \text{ value} = 0.57, \quad \text{GFI} = 1, \quad \text{AGFI} = 0.98, \quad \text{SRMR} = 0.008.$$

Inadmissble solutions have been observed for all data sets except data set no. 2, for which the estimation procedure failed to converge to a solution.

S1.1.3 The result of fitting the CFA(7, 6) model to the Europe data

Supported by the preliminary estimates of α_f:s, all modified version of the CFA(7, 6) model were estimated under the restriction $Lsim = Osim = 0$, which also required setting all associated correlation coefficients to zero. A positive consequence of these restrictions is that it gives us more degrees of freedom. The modified CFA model with the best overall model fit is shown in Table S1.1.3.

Table S1.1.3. Estimated parameters of the modified version of the CFA(7, 6) model fitted to the Europe data.

• *The result for data set no. 1*

Parameter	Estimate	p value	Parameter	Estimate	p value	Parameter	Estimate	p value
Ssim	0.047	1.1e–05	$\sigma^2_{\eta_{\text{internal pseudo}}}$	0.0227	3.1e–09	$\sigma_{\tilde{\delta}_{\text{Land (anthr)}}\,\tilde{\delta}_{\text{Volc}}}$	0.0029	0.039
Vsim	0.137	4.3e–32	$\sigma_{\tilde{\delta}_{\text{Sol}}\,\tilde{\delta}_{\text{GHG}}}$	0.0017	0.11	$\sigma_{\tilde{\delta}_{\text{Land (anthr)}}\,\tilde{\delta}_{\text{comb}}}$	0.0047	1.7e–03
Gsim	0.050	7.4e–07	$\sigma_{\tilde{\delta}_{\text{Land (anthr)}}\,\tilde{\delta}_{\text{Orb}}}$	0.0016	0.086	$\sigma_{\tilde{\delta}_{\text{Land (anthr)}}\,\eta_{\text{internal pseudo}}}$	0.0041	0.027

To assess the overall model fit:

$$\text{Model } \chi^2 = 9.4, \quad \text{df} = 19, \quad p \text{ value} = 0.97, \quad \text{GFI} = 0.97, \quad \text{AGFI} = 0.96, \quad \text{SRMR} = 0.067.$$

• *Summary of the results based on all 7 data sets*

	Min	Mean	Max		Min	Mean	Max		Min	Mean	Max
$\widehat{Ssim}$	0.038	0.043	0.047	$\widehat{\sigma}_{\tilde{\delta}_{\text{Land (anthr)}}\,\tilde{\delta}_{\text{Orb}}}$	0.0015	0.0018	0.0020	Model χ^2	9.4	13.5	18.8
$\widehat{Vsim}$	0.136	0.137	0.139	$\widehat{\sigma}_{\tilde{\delta}_{\text{Land (anthr)}}\,\tilde{\delta}_{\text{Volc}}}$	0.0026	0.0028	0.0029	p value	0.47	0.78	0.97
$\widehat{Gsim}$	0.046	0.049	0.050	$\widehat{\sigma}_{\tilde{\delta}_{\text{Land (anthr)}}\,\tilde{\delta}_{\text{comb}}}$	0.0047	0.0057	0.0067	GFI	0.95	0.96	0.97
$\widehat{\sigma}^2_{\eta_{\text{internal pseudo}}}$	0.0227	0.0249	0.0306	$\widehat{\sigma}_{\tilde{\delta}_{\text{Land (anthr)}}\,\eta_{\text{internal pseudo}}}$	0.0015	0.0018	0.0020	AGFI	0.93	0.95	0.96
$\widehat{\sigma}_{\tilde{\delta}_{\text{Sol}}\,\tilde{\delta}_{\text{GHG}}}$	0.0016	0.0016	0.0017					SRMR	0.063	0.072	0.089

The solution for each data set is admissible.

According to Table S1.1.3, the estimation resulted in an admissible solution for each data set. Furthermore, the overall fit of the model is quite good both statistically and heuristically. For example, for data set no. 1, p value for the χ^2 statistic, 0.97, is much larger than 0.05, GFI $= 0.97 > 0.9$, AGFI $= 0.96 > 0.80$, and finally SRMR $= 0.067 < 0.08$. The model also demonstrated a stable performance across all seven data sets both in terms of the parameter estimates and in terms of its overall fit to the data.

Further, the parameter estimates seem to be interpretable from the climatological point of view. The effect of the solar, volcanic and GHG forcings on the simulated summer mean temperature in Europe during the period 850–1849 AD is estimated as significant. For example, for data set no. 1, the following estimates were observed: $\widehat{Ssim} = 0.047$ with p value$= 1.1e{-}05$, $\widehat{Vsim} = 0.137$ with p value$= 4.3e{-}32$, and $\widehat{Gsim} = 0.050$ with p value$= 7.4e{-}07$. Comparing $\widehat{Ssim}$, $\widehat{Vsim}$ and $\widehat{Gsim}$ to each other, one can conclude that the magnitude of the influence of the volcanic forcing is more than twice as large as that of the solar and GHG forcings. Recall from LAS22num that coefficients in CFA and SEM models are standardised, which makes comparisons between them meaningful.

Concerning the parameter *Gsim*, the presented CFA model tells us that *Gsim* represents the effect of anthropogenic changes in the reconstructed GHG forcing. This conclusion is motivated by the fact that ξ^S_{GHG} is not related to the temperature responses to the natural forcings, here ξ^S_{Sol} and ξ^S_{Volc}. Climatologically, the significant effect of anthropogenic changes in the GHG forcing can be justified by an effect in the last about one century of data in the analysed period.

However, it deserves to be noted that the effect of the solar forcing seems to be underestimated for all seven data sets. The underestimation could be seen in the normalised residuals (the matrix with the normalised residuals is not shown here).

Prior to drawing final conclusions, let us investigate the underlying latent structure of the data by means of the SEM model.

S1.1.4 The result of fitting the SEM model to the Europe data

The path diagram of the resulting SEM model is shown in Fig. S1.1.1. As one can see, the SEM model, just as the CFA model above, hypothesises that the land use and orbital forcings have a negligible effect on the simulated summer mean temperature in Europe during 850–1849 AD. Therefore, both statistical models do not contain the forced components $\xi^S_{\mathrm{Land\,(anthr)}}$ and ξ^S_{Orb}, meaning that $x_{\mathrm{Land\,(anthr)}}$ and x_{Orb} represent the internal temperature variability generated by the corresponding single-forcing climate model. That is, $x_{\mathrm{Land\,(anthr)}} = \tilde{\delta}_{\mathrm{Land\,(anthr)}}$ and $x_{\mathrm{Orb}} = \tilde{\delta}_{\mathrm{Orb}}$.

However, unlike the CFA model, the SEM model contains two new observable variables, not presented even in the initial SEM model described in LAS22num. The variables are $x^+_{\mathrm{Land\,(anthr)}}$ and x^+_{Orb}. They were constructed in an analogous way and for the same reason as $x^+_{\mathrm{Land\,(anthr)}}$ within the SEM model fitted to the North America data (see LAS22num). For the convenience of the reader, let us repeat here our way of reasoning.

So, initially, $x^+_{\mathtt{f}}$, where $\mathtt{f} \in \{\mathrm{Land\,(anthr)}, \mathrm{Orb}\}$, is constructed by equating it to the original $x_{\mathtt{f}}$ by setting the disturbance variance of $x^+_{\mathtt{f}}$ to zero, and by relating it to $x_{\mathtt{f}}$ through the regression coefficient equal to 1. Note that in the presence of $x^+_{\mathtt{f}}$ in the model, the corresponding $x_{\mathtt{f}}$ is viewed as latent.
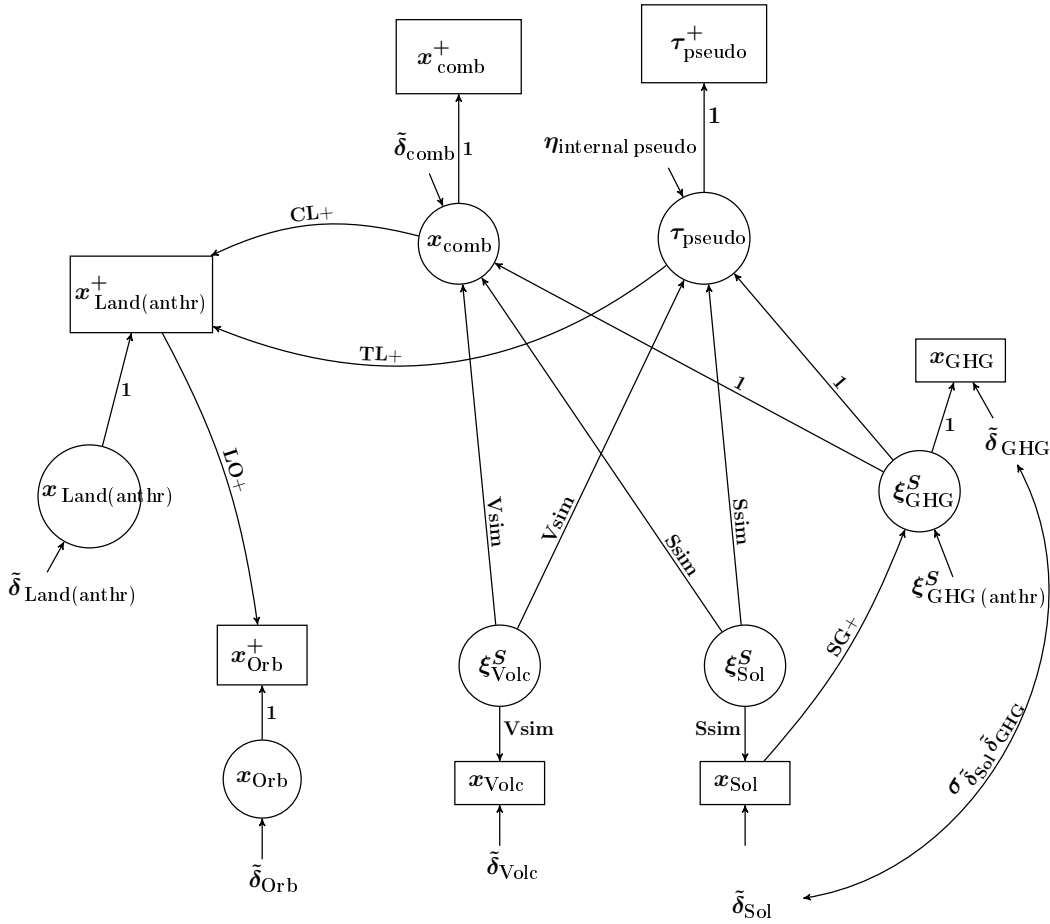
Figure S1.1.1. Path diagram of the modified SEM model fitted to the Europe data.

As known, under the CFA model specification, specific factors, representing within our framework the internal random temperature variability, can be statistically related only to each other, and only by means of covariances. Within the CFA model above (see Table S1.1.3), $\tilde{\delta}_{\text{Land(anthr)}}$ is related in this way to $\tilde{\delta}_{\text{Orb}}$, $\tilde{\delta}_{\text{comb}}$ and to $\eta_{\text{internal pseudo}}$, each of which represents the internal temperature variability, generated by the corresponding climate model.

However, it turned out that a better overall model fit can be achieved if $x_{\text{Land(anthr)}}$ receives a causal input from x_{comb} and τ_{pseudo}, respectively. Statistically, these inputs relate $\tilde{\delta}_{\text{Land(anthr)}}$ not only to $\tilde{\delta}_{\text{comb}}$ and $\eta_{\text{internal pseudo}}$, but also to the forced temperature variability, represented by ξ^S_{Sol}, ξ^S_{Volc} and ξ^S_{GHG}.

Although no dynamical relationships between the reconstructions of the forcings and the internal processes were implemented in the climate modelling experiment under consideration, the causal inputs to $x_{\text{Land(anthr)}}$ can be viewed as a statistical

Table S1.1.4. The result of estimating the SEM model presented graphically in Fig. S1.1.1 (region: Europe).

• *The result for data set no. 1*

Parameter	Estimate	p value	Parameter	Estimate	p value	Parameter	Estimate	p value
$Ssim$	0.054	$7.5e{-}06$	$CL+$	0.157	0.017	$\mathrm{Var}(\xi^S_{\mathrm{GHG\,(anthr)}})$	0.0028	0.014
$Vsim$	0.137	$1.3e{-}31$	$TL+$	0.024	0.65	$SG+$	-0.149	0.28
$\sigma^2_{\eta_{\mathrm{internal\,pseudo}}}$	0.023	$4.7e{-}09$	$LO+$	0.244	0.030	$\sigma_{\tilde{\delta}_{\mathrm{Sol}}\,\tilde{\delta}_{\mathrm{GHG}}}$	0.0030	0.10

$$\sqrt{\widehat{\mathrm{Var}}(\xi^S_{\mathrm{GHG}})} = \widehat{Gsim}_{SEM} = \sqrt{(\widehat{SG+})^2 \cdot \left(\widehat{Ssim}^2 + \sigma^{2\,*}_{\tilde{\delta}_{\mathrm{Sol}}}\right) + \widehat{\mathrm{Var}}(\xi^S_{\mathrm{GHG\,(anthr)}})} = 0.057 \ (p \text{ value} = 0.030)$$

To assess the overall model fit:

$$\text{Model } \chi^2 = 6.09, \quad \text{df} = 19, \quad p \text{ value} = 0.998, \quad \text{GFI} = 0.98, \quad \text{AGFI} = 0.98, \quad \text{SRMR} = 0.044.$$

• *Summary of the results based on all 7 data sets*

	Min	Mean	Max		Min	Mean	Max		Min	Mean	Max
$\widehat{Ssim}$	0.048	0.052	0.054	$\widehat{\sigma}_{\tilde{\delta}_{\mathrm{Sol}}\,\tilde{\delta}_{\mathrm{GHG}}}$	0.0031	0.0034	0.0036	Model χ^2	6.10	12.2	15.6
$\widehat{Vsim}$	0.134	0.136	0.139	$\widehat{SG+}$	-0.195	-0.170	-0.140	p value	0.69	0.84	1.00
$\widehat{Gsim}_{SEM}$	0.057	0.058	0.060	$\widehat{CL+}$	0.049	0.168	0.244	GFI	0.96	0.97	0.98
$\widehat{\sigma}^2_{\eta_{\mathrm{internal\,pseudo}}}$	0.023	0.025	0.030	$\widehat{TL+}$	-0.004	0.050	0.168	AGFI	0.94	0.95	0.98
$\widehat{\mathrm{Var}}(\xi^S_{\mathrm{GHG\,(anthr)}})$	0.0028	0.0030	0.0032	$\widehat{LO+}$	0.24	0.24	0.24	SRMR	0.044	0.055	0.069

The solution for each data set is admissible.

An important note on Table S1.1.4 is that $\sigma^{2\,*}_{\tilde{\delta}_{\mathrm{Sol}}}$ denotes the variance of the mean sequence $\bar{x}_{\mathrm{Sol}}$, i.e. $\sigma^{2\,*}_{\tilde{\delta}_{\mathrm{Sol}}}$ is in effect $\sigma^{2\,*}_{\tilde{\delta}_{\mathrm{Sol}}}/k_{\mathrm{Sol}}$, where $k_{\mathrm{Sol}}=2$ and $\sigma^{2\,*}_{\tilde{\delta}_{\mathrm{Sol}}}$ is estimated a priori by means of our estimator (3) from LAS22num. Since we do not use the bar notation to designate the mean sequences (see Sect.3 in LAS22num), it is motivated to apply a conformable notation for their variances. Similar notations are applied throughout the rest of the Supplement.

145 description of complicated climatological processes, which may occur in the real-world climate system and which may be reflected both in the forcing reconstructions and in the physical basis for the internal processes that are implemented in the climate model.

Indeed, in the real-world climate system, the causal inputs to $x_{\mathrm{Land\,(anthr)}}$ could arise as a result of various interactions, or equivalently climate feedback mechanisms, occuring in the climate system, namely (i) interactions between the internal pro-
150 cesses and the forcings, in particular the volcanic, solar and GHG forcings, and (ii) interactions between the internal processes themselves. Let us note that statistically, the co-relation between $x_{\mathrm{Land\,(anthr)}}$ and x_{comb} (or τ_{pseudo}) could also be analysed by means of the input from $x_{\mathrm{Land\,(anthr)}}$ to x_{comb}, but it is difficult to accept that in the real-world climate system, the internal processes may be a cause of the variations in the external forcings, in particular the solar and volcanic forcings.

A disadvantage of letting x_{comb} and τ_{pseudo} influence $x_{\mathrm{Land\,(anthr)}}$ is that it would change the interpretation of the latter from
155 the climate modelling perspective. More precisely, this would mean that $x_{\mathrm{Land\,(anthr)}}$ was generated by the climate model driven by the volcanic, solar and GHG forcings, which is not the case. Therefore, our goal is to formulate a SEM model, which, on one hand, unambiguously indicates that $x_{\mathrm{Land\,(anthr)}}$ was generated by the $x_{\mathrm{Land\,(anthr)}}$ climate model, and, on the other hand, links $x_{\mathrm{Land\,(anthr)}}$ to other model variables generated by other climate models analysed. This goal can be achieved by creating a new

9

variable, representing a copy of $x_{\text{Land (anthr)}}$, and let x_{Volc} influence this new variable instead of $x_{\text{Land (anthr)}}$. In Fig. S1.1.1, the associated regression coefficients correspond to the paths *CL+* and *TL+*, respectively.

One can also see in Fig. S1.1.1 that the paths *CL+* and *TL+* go through $x^{+}_{\text{Land (anthr)}}$ further to x^{+}_{Orb}, or equivalently $\tilde{\delta}_{\text{Orb}}$, along the path *LO+*. Hence, the SEM model relates not only $\tilde{\delta}_{\text{Land (anthr)}}$, but also $\tilde{\delta}_{\text{Orb}}$ to the forced and internal temperature variations, embedded in x_{comb} and τ_{pseudo}. The main advantage of using regressions in this case is that a large number of observed covariances could be statistically explained by estimating a smaller number of parameters. More precisely, 11 (nonduplicated) observed covariances, namely $\text{cov}(x^{+}_{\text{Land (anthr)}}, x^{+}_{\text{Orb}})$, $\text{cov}(x^{+}_{\text{f}}, x_{\text{comb}})$, $\text{cov}(x^{+}_{\text{f}}, \tau_{\text{pseudo}})$, $\text{cov}(x^{+}_{\text{f}}, x_{\text{Volc}})$, $\text{cov}(x^{+}_{\text{f}}, x_{\text{Sol}})$, $\text{cov}(x^{+}_{\text{f}}, x_{\text{GHG}})$, where $\text{f} \in \{\text{Land (anthr)}, \text{Orb}\}$, were explained by means of three parameters: *CL+*, *TL+*, and *OL+*. As a result, a better overall model fit was achieved without losing 11 degrees of freedom but only three.

An additional improvement in the model overall fit was achieved by freeing the causal input from x_{Sol} to ξ^{S}_{GHG}, denoted *SG+*. In the real-world climate system, this input can be associated with interactions between the concentrations of greenhouse gases in the atmosphere and the climate system (in particular the solar forcing and the internal processes), which may be reflected in the reconstructed GHG forcing history used to drive the climate model under consideration. Based on the estimates of *SG+*, presented in Table S1.1.4, we may say that the natural component in the overall temperature response to the reconstructed GHG forcing is not well seen in the simulated summer mean temperature in Europe during $850-1849$ AD. For example, for data set no. 1, $\widehat{SG+} = -0.132$ with p value$= 0.33$.

The path *SG+* also tells us that the solar forcing exerts not only a direct influence, represented by the parameter *Ssim*, but also an indirect influence, represented by the product *Ssim·SG+*. The sum of the direct and indirect effects gives a total effect. Although, it would of great interest to provide estimates of indirect and total effects, we refrain from such calculations. As explained in LAS22num, the aim of the present analysis is to compare the performance of three statistical models, two of which are capable of estimating only direct effects. In addition, it is not possible to provide within the confines of the present analysis the complete theoretical background of calculating indirect and total effects, which can arise in SEM models of different degrees of complexity. Therefore, we here focus only on the estimation and comparison of direct effects, provided by the three statistical model under consideration.

Turning back to the estimates provided by the SEM model, we note that the estimate of $\text{Var}(\xi^{S}_{\text{GHG (anthr)}})$ is significant for data set no. 1 ($\widehat{\text{Var}}(\xi^{S}_{\text{GHG (anthr)}}) = 0.0028$ with the associated p value of 0.014). Together with the insignificant estimates of *SG+*, this result suggests that the effect of anthropogenic global-scaled variations, which may be reflected in the actual reconstruction of the GHG forcing, is better pronounced in the simulated summer mean temperature in Europe during $850-1849$ AD than the effect of natural global-scaled variations. Importantly, the same conclusion has been suggested by the CFA model above.

The overall effect of (anthropogenic and natural variations in) the GHG forcing is represented by the parameter $\widehat{Gsim_{SEM}}$, which is the standard deviation of ξ^{S}_{GHG}, calculated afterwards by means of the delta method described here in Sect.S2.5. For data set no. 1, $Gsim_{SEM}$ is estimated to be 0.057 with the associated p value of 0.03. A similar result was observed for the remaining data sets as well. Thus, we may say that the SEM model detects a moderately significant overall effect of anthropogenic and natural changes in the GHG forcing in the simulated summer mean temperature in Europe during $850-1849$ AD.

Concerning the effect of the volcanic and solar forcing, the SEM model, just as the CFA model above, suggests that the effect of the volcanic forcing is estimated as the largest and the most significant compared to the effect of the solar forcing (see, for example the result for data set no. 1: $\widehat{Ssim} = 0.054$ with p value$= 7.5e{-}06$, $\widehat{Vsim} = 0.137$ with p value$= 1.3e{-}31$).

S1.1.5 Summary and conclusion (region: Europe)

The first statistical model, the ME-CFA(6, 5) model, has to be rejected due to inadmissble solutions.

In contrast to the ME-CFA(6, 5) model, the CFA and SEM models have admissible and climatologically defensible solutions. Importantly, in terms of the direct effects of the forcings, the interpretations of both statistical models are basically the same (see the overview in Table 9 in LAS22num). In addition, both models demonstrated a stable performance across all seven data sets.

Nevertheless, the SEM model fits the data better than the CFA model, albeit both statistical models have the same number of degrees of freedom (df=19). The better fit of the SEM model is especially reflected in the smaller SRMR values than those observed for the CFA model. Compare the observed range of the SRMR values for the CFA model, (min(SRMR)=0.063, mean(SRMR)=0.072, max(SRMR)=0.089), to the corresponding range observed under the SEM model: (min(SRMR)=0.044, mean(SRMR)=0.065, max(SRMR)=0.069). Motivated by the better overall model fit of the SEM model, our suggestion is to choose the SEM model as a statistically adequate and climatologically defensible approximation of the underlying latent structure of the Europe data.

S1.2 The Arctic (annual mean temperature)

The data analysed are presented in Table S1.2.1, from which it follows that five data sets were analysed. Results for the three statistical models of interest are provided in Tables S1.2.2 - S1.2.4.

Table S1.2.1. Overview of replicates of each x_f, used to construct five regional Arctic data sets (annual mean temperature). Each data set contains different $\bar{x}_{\text{comb}}$ and τ_{pseudo}, where $\bar{x}_{\text{comb}}$ is constructed by averaging over four replicates randomly selected from the four that remained after $x_{\text{comb repl}.i}$:s, $i = 1, 3, 6, 8, 10$, have been eliminated and after one of $x_{\text{comb repl}.i}$:s, $i = 2, 4, 5, 7, 9$, is chosen to represent τ, i.e. τ_{pseudo}.

		Mean sequences				
Data set	x_{Sol},	$x_{\text{Orb}}, x_{\text{GHG}}$,	$x_{\text{Land (anthr)}}$	x_{Volc}	x_{comb}	$x_{\text{comb repl}.i} = \tau_{\text{pseudo}}$
1	1,3,4	all associated repl's	1,3	1,2	4,7	2
2	1,3,4	all associated repl's	1,3	1,2	5,9	4
3	1,3,4	all associated repl's	1,3	1,2	2,7	5
4	1,3,4	all associated repl's	1,3	1,2	4,9	7
5	1,3,4	all associated repl's	1,3	1,2	2,4	9

S1.2.1 Preliminary analyses of final single-forcing ensembles by means of the CFA(k_f, 1) model

Each single-forcing ensemble in Table S1.2.1 was analysed by means of the CFA(k_f, 1) model.

When analysing the $x_{\text{Land (anthr)}}$ ensemble, the CFA($k_f = 2$, 1) model was estimated under the restriction $Lsim = 0$, which corresponds to hypothesising that the effect of anthropogenic changes in the land-use forcing is not detectable in the simulated annual mean temperature in the Arctic during the period of study. The hypothesis is motivated by the reconstruction of the land-use forcing, which does not show any variability over the Arctic on an annual basis during the analysis period (see Fig. S4.5 in Fetisova et al., 2017). It turned out that there was no reason to reject this hypothesis because the resulting the CFA($k_{\text{Land (anthr)}}$,0) model fitted the data well both statistically and heuristically (the result is not presented here).

Concerning the remaining forcings, the results suggested that the effects of the solar, orbital, volcanic and GHG forcings are well detectable in the simulated annual mean temperature in the Arctic during $850 - 1849$ AD ($\widehat{\alpha}_{\text{Sol}} = 0.097$ with p value$= 2.1e{-}04$, $\widehat{\alpha}_{\text{Orb}} = 0.0932$ with p value$= 0.0024$, $\widehat{\alpha}_{\text{Volc}} = 0.202$ with p value$= 3.4e{-}19$, and $\widehat{\alpha}_{\text{GHG}} = 0.113$ with p value$= 5.4e{-}06$). Once again, let us emphasise that analysing the x_{GHG} ensemble without combining it with the ensembles, associated with other forcings, does not make it possible to get any idea about the character of the GHG forcing.

S1.2.2 The result of fitting the ME-CFA(6, 5) model to the Arctic data

According to Table S1.2.2, the ME-CFA(6, 5) model has demonstrated an unstable performance across the five data sets available. For the three data sets, the model could be rejected either due to the nonconvergence of the estimation procedure (Data sets no. 1 and 2) or due to an unacceptable fit (data set no. 3, for which both the p value for the χ^2 statistic, 0.012, was

230 quite low, and AGFI $= 0.62$ was less then the recommended cutoff value of 0.8). All these together makes it doubtful to accept the ME-CFA(6, 5) model as an appropriate and adequate description of the underlying structure of the data even if the model could be accepted for the two of the five data sets.

Table S1.2.2. The result of estimating the ME-CFA(6, 5) model, fitted to the Arctic data.

- *The result for data set no. 3*

Parameter	Estimate	p value	Parameter	Estimate	p value
Ssim	0.101	1.2e–05	ϕ_{SO}	0.49	0.15
Strue	-0.084	0.55	ϕ_{SV}	0.25	0.33
Osim	0.101	1.0e–04	ϕ_{SL}	0.41	0.33
Otrue	0.118	0.31	ϕ_{SG}	0.54	0.72
Vsim	0.203	3.1e–12	ϕ_{OV}	0.41	0.12
Vtrue	0.083	0.55	ϕ_{OL}	0.21	0.64
Lsim	0.100	0.01	ϕ_{OG}	0.19	0.57
Ltrue	0.113	0.47	ϕ_{VL}	0.57	0.11
Gsim	0.111	1.9e–06	ϕ_{VG}	0.12	0.61
Gtrue	0.034	0.80	ϕ_{LG}	0.40	0.33

To assess the overall model fit:

Model $\chi^2 = 6.3$, df $= 1$, p value $= 0.012$, GFI $= 0.98$, AGFI $= 0.62$, SRMR $= 0.042$.

The estimation procedure failed to converge to a solution for Data sets no. 1 and 2. For Data sets no. 3, 4 and 5, the solution is admissible. For the last two data sets, the model could be accepted both statistically and heurustically.

S1.2.3 The result of fitting the CFA(7, 6) model to the Arctic data

Even the CFA model has demonstrated a highly unstable performance, which could be explained by a substantial variability in
235 the estimates of several specific-factor covariances across the five data sets available. For example, the estimate of $\sigma_{\tilde{\delta}_{\text{Land (anthr)}}\,\tilde{\delta}_{\text{comb}}}$ was significant for Data set no. 3, but for the other four data sets the estimate was clearly insignificant. In order to avoid the nonconvergence of the estimation procedure, only some specific-factor covariances, which turned out to be significant only for one data set, could be freed up for all data sets. As a result, no version of the basic CFA model demonstrated an adequate fit to the data.

240 As an example, consider the CFA model, presented in Table S1.2.3. Although this model demonstrated the most stable performance and the best overall fit among several CFA models, one can see that its overall fit is quite poor, especially in terms of the SRMR values. More precisely, the range of the observed SRMR values exceed the recommended cutoff value of 0.08 (min(SRMR)=0.091, max(SRMR)=0.100).

At the same time, the modification indices indicated that an improvement of the model fit is possible by freeing up some
245 causal inputs to ξ_{GHG}^{S}. Therefore, let us investigate the structure of the data by means of the SEM specification.

Table S1.2.3. Estimates of the first modified version of the CFA(7, 6) model fitted to the Arctic data.

● *The result for data set no. 5*

Parameter	Estimate	p value	Parameter	Estimate	p value	Parameter	Estimate	p value
$Ssim$	0.088	1.5e–05	ϕ_{SG}	0.34	0.38	$\sigma^2_{\eta_{\text{internal pseudo}}}$	0.063	1.3e–09
$Osim$	0.081	2.9e–04	$\sigma_{\tilde{\delta}_{\text{Sol}}\,\tilde{\delta}_{\text{Land (anthr)}}}$	0.0045	0.21	$\sigma_{\tilde{\delta}_{\text{Land (anthr)}}\,\tilde{\delta}_{\text{comb}}}$	-0.0016	0.82
$Vsim$	0.206	5.8e–20	$\sigma_{\tilde{\delta}_{\text{Sol}}\,\tilde{\delta}_{\text{Orb}}}$	0.0047	0.14	$\sigma_{\tilde{\delta}_{\text{Land (anthr)}}\,\eta_{\text{internal pseudo}}}$	0.013	0.12
$Gsim$	0.083	1.5e–05	$\sigma_{\tilde{\delta}_{\text{Land (anthr)}}\,\tilde{\delta}_{\text{Volc}}}$	0.0093	0.12			

To assess the overall model fit:

$$\text{Model } \chi^2 = 22.8, \quad \text{df} = 17, \quad p \text{ value} = 0.15, \quad \text{GFI} = 0.95, \quad \text{AGFI} = 0.91, \quad \text{SRMR} = 0.091.$$

● *Summary of the results based on all 5 data sets*

	Min	Mean	Max		Min	Mean	Max		Min	Mean	Max
$\widehat{Ssim}$	0.071	0.084	0.089	$\widehat{\sigma}_{\tilde{\delta}_{\text{Sol}}\,\tilde{\delta}_{\text{Land (anthr)}}}$	0.0043	0.0049	0.0060	Model χ^2	19.0	24.1	29.0
$\widehat{Osim}$	0.081	0.089	0.100	$\widehat{\sigma}_{\tilde{\delta}_{\text{Sol}}\,\tilde{\delta}_{\text{Orb}}}$	0.0047	0.0049	0.0054	p value	0.03	0.15	0.33
$\widehat{Vsim}$	0.188	0.199	0.206	$\widehat{\sigma}_{\tilde{\delta}_{\text{Land (anthr)}}\,\tilde{\delta}_{\text{Volc}}}$	0.0083	0.0089	0.0095	GFI	0.92	0.94	0.95
$\widehat{Gsim}$	0.073	0.078	0.083	$\widehat{\sigma}_{\tilde{\delta}_{\text{Land (anthr)}}\,\tilde{\delta}_{\text{comb}}}$	-0.0016	0.0054	0.0173	AGFI	0.88	0.90	0.92
$\widehat{\phi}_{SG}$	0.07	0.25	0.34	$\widehat{\sigma}_{\tilde{\delta}_{\text{Land (anthr)}}\,\eta_{\text{internal pseudo}}}$	0.0003	0.0082	0.0220	SRMR	0.091	0.094	0.100
$\widehat{\sigma}^2_{\eta_{\text{internal pseudo}}}$	0.064	0.077	0.096								

The solution for each data set is admissible.

S1.2.4 The result of fitting the SEM model to the Arctic data

The path diagram of the resulting SEM model is depicted in Fig. S1.2.1. The first thing to note is that the SEM model, just as the CFA model above, hypothesises that the land-use forcing has a negligible effect on the simulated summer mean temperature in Europe during 850–1849 AD. That is, neither statistical model contains the forced component $\xi^S_{\text{Land (anthr)}}$, meaning that $x_{\text{Land (anthr)}}$ represents the internal temperature variability generated by the $x_{\text{Land (anthr)}}$ climate model. In terms of the model variables, it means that $x_{\text{Land (anthr)}} = \tilde{\delta}_{\text{Land (anthr)}}$.

However, unlike the CFA model, the SEM model contains a new observable variable, denoted $x^+_{\text{Land (anthr)}}$. The variable was constructed in the same way and for the same reason as the variable $x^+_{\text{Land (anthr)}}$ in the SEM model applied to the Europe data (for the details, see Sect.1.1. and Fig. S1.1.1).

Prior to discussing their interpretation, let us evaluate the overall model fit. Based on Table S1.2.4, we may conclude that the SEM model fits all data sets well both statistically and heuristically. For example, for data set no. 5, for which the model was initially formulated, the p value for the χ^2 statistic, 0.58, is much larger than 0.05, GFI $= 0.96 > 0.9$, AGFI $= 0.94 > 0.80$, and finally SRMR $= 0.072 < 0.08$. For the sake of comparison, let us examine the corresponding result for the CFA model in Table S1.2.3: the p value$= 0.15$, GFI $= 0.95$, AGFI $= 0.91$, and SRMR $= 0.091$. Taking into account that both models have the same number of degrees of freedom (df$= 17$), this comparison indicates that the SEM specification is more appropriate for the data analysed than the CFA specification. However, prior to drawing final conclusions, the interpretation of the SEM model needs to be discussed.

As one can see in Fig. S1.2.1, $x^+_{\text{Land (anthr)}}$ receives three causal inputs: the input $CL+$ from x_{comb}, the input $TL+$ from τ_{pseudo}, and the input $SL+$ from ξ^S_{Sol}. These inputs tell us that the internal temperature variability, generated by the $x_{\text{Land (anthr)}}$ climate

265 model, exhibits a co-relation with the forced temperature variability, associated with the solar, volcanic, orbital and GHG forcings, and with the internal temperature variability (generated by the multi-forcing climate model). In the real-world climate system, such co-relations are quite expected because they may arise as a result of interactions between the internal processes and the climate system, which may be reflected in the forcing reconstructions and the theoretical physical basis of internal processes, implemented in the climate model under consideration. Although no dynamical relationships between the internal

270 processes and the forcings are implemented in the climate model under study, observing these co-relations in the simulated climate system, in our opinion, speaks in favor of the climate model under consideration, in particular the forcing reconstructions and the theoretical physical basis of internal processes, implemented in this climate model.
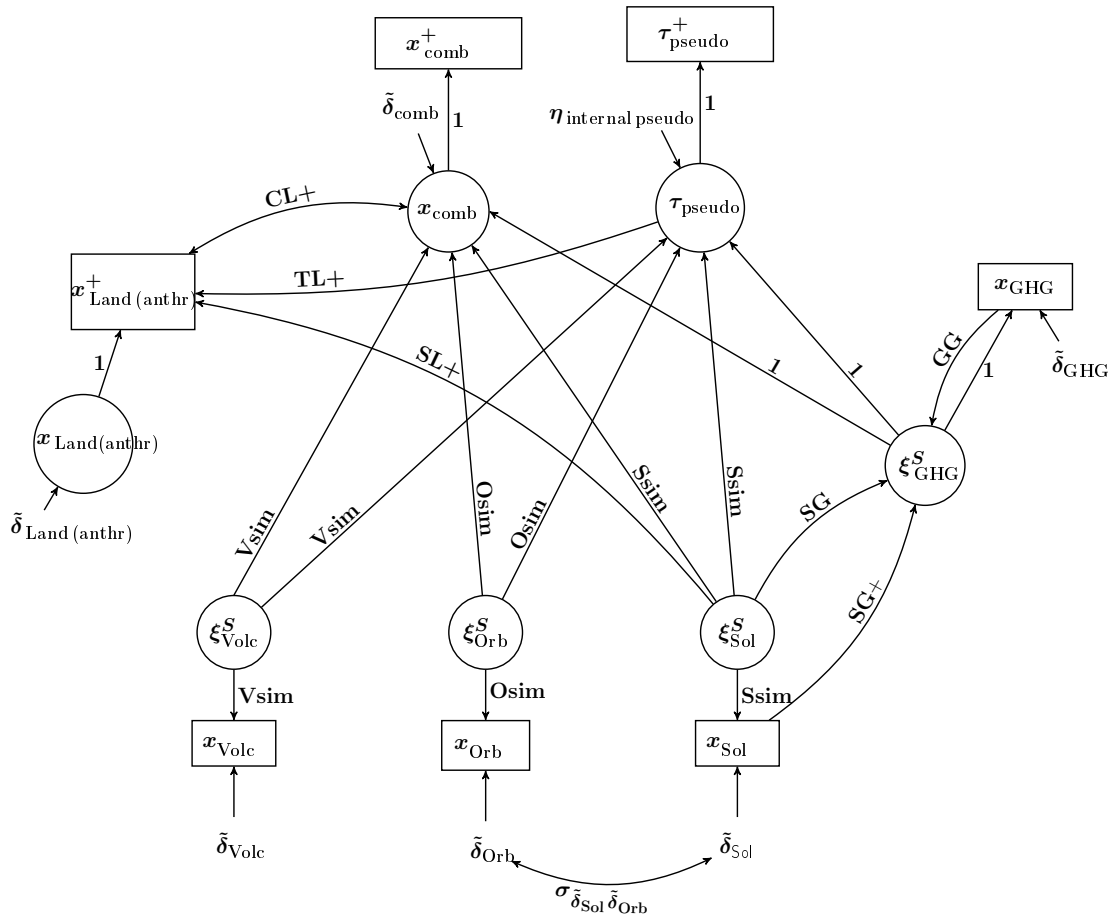

Figure S1.2.1. Path diagram of the SEM model fitted to the *Arctic* data.

Table S1.2.4. The result of estimating the SEM model presented graphically in Fig. S1.2.1 (region: the Arctic).

● *The result for data set no. 5*

Parameter	Estimate	p value	Parameter	Estimate	p value	Parameter	Estimate	p value
$Ssim$	0.091	$5.5e{-}06$	GG	0.109	0.72	$SL{+}$	0.024	0.52
$Osim$	0.082	$1.5e{-}04$	$SG{+}$	0.420	0.44	$CL{+}$	-0.059	0.48
$Vsim$	0.211	$9.9e{-}23$	SG	-0.084	0.60	$TL{+}$	0.130	0.04
$\sigma^2_{\eta_{\text{internal pseudo}}}$	0.098	$1.9e{-}09$				$\sigma_{\tilde{\delta}_{\text{Sol}}\,\tilde{\delta}_{\text{Orb}}}$	0.0053	0.096

$$\sqrt{\widehat{\text{Var}}(\xi^S_{\text{GHG}})} = \widehat{Gsim}_{SEM} = \sqrt{\left((\widehat{SG{+}})^2 \cdot (\widehat{Ssim}^2 + \sigma^{2*}_{\tilde{\delta}_{\text{Sol}}}) + \widehat{SG}^2 + \widehat{GG}^2 \cdot \sigma^{2*}_{\tilde{\delta}_{\text{GHG}}}\right)/(1-\widehat{GG})^2} = 0.127 \quad (p\,\text{value} = 0.79)$$

To assess the overall model fit:

Model $\chi^2 = 15.22$,   df $= 17$, p value $= 0.58$,   GFI $= 0.96$,   AGFI $= 0.94$,   SRMR $= 0.068$.

● *Summary of the results based on all 5 data sets*

	Min	Mean	Max		Min	Mean	Max		Min	Mean	Max
$\widehat{Ssim}$	0.078	0.087	0.093	$\widehat{SL{+}}$	0.022	0.031	0.042	Model χ^2	12.4	16.5	21.3
$\widehat{Osim}$	0.082	0.091	0.104	$\widehat{CL{+}}$	-0.069	0.045	0.244	p value	0.21	0.50	0.78
$\widehat{Vsim}$	0.191	0.203	0.211	$\widehat{TL{+}}$	-0.099	0.055	0.222	GFI	0.94	0.96	0.97
$\widehat{GG}$	0.079	0.106	0.151	$\widehat{\sigma}_{\tilde{\delta}_{\text{Sol}}\,\tilde{\delta}_{\text{Orb}}}$	0.0053	0.0058	0.0066	AGFI	0.90	0.93	0.94
$\widehat{SG{+}}$	0.300	0.370	0.430	$\widehat{\sigma}^2_{\eta_{\text{internal pseudo}}}$	0.067	0.079	0.098	SRMR	0.068	0.071	0.076
$\widehat{SG}$	-0.089	-0.077	-0.057	$\widehat{Gsim}_{SEM}$	0.097	0.114	0.128				

The solution for each data set is admissible.

Further, according to Fig. S1.2.1, the SEM model also suggests co-relations which may be viewed as a counterpart of real-world interactions between the concentrations of greenhouse gases in the atmosphere and the climate system. These co-relations are represented by the inputs from ξ^S_{Sol}, x_{Sol}, and x_{GHG} to ξ^S_{GHG} (see the path denoted SG, $SG{+}$ and GG, respectively). Although according to Table S1.2.4 the estimates of these parameters are not significant, freeing up these paths contributed to a better explanation of several observed variances and covariances, e.g. $\text{var}(x_{\text{Sol}})$, $\text{var}(x_{\text{GHG}})$, $\text{cov}(x_{\text{Sol}}, x_{\text{GHG}})$, $\text{cov}(x_{\text{Sol}}\, x_{\text{comb}})$, $\text{cov}(x_{\text{Sol}}, \tau_{\text{pseudo}})$, $\text{cov}(x_{\text{GHG}}, x_{\text{comb}})$, $\text{cov}(x_{\text{GHG}}, \tau_{\text{pseudo}})$, $\text{cov}(x_{\text{Land (anthr)}}, x_{\text{comb}})$, $\text{cov}(x_{\text{GHG}}, \tau_{\text{pseudo}})$.

The insignificance of these paths also led to an insignificant estimate of $Gsim_{SEM}$, representing the standard deviation of ξ^S_{GHG} and calculated afterwards. For example, for data set no. 5, $Gsim_{SEM}$ is estimated to be 0.127 with the associated p value of 0.79. This result suggests that the overall (direct) effect of global-scaled variations in the Ghg forcing is not detected in the simulated annual mean temperature in the Arctic during the period of the study. Here, we would like to emphasise that the analysis of the x_{GHG} ensemble by means of the CFA(k_{GHG}, 1) model suggested the opposite conclusion. Recall from the beginning of this section that the estimate of α_{GHG}, provided by the CFA(k_{GHG}, 1) model, was highly significant. A possible explanation for this difference could be that the CFA(k_{GHG}, 1) model is a model with much fewer parameters, so it is not unreasonable for the estimate of α_{GHG} to absorb information from different parameters in the larger model, for example GG, $SG{+}$ and SG.

It is also worth noting that the SEM model does not contain the disturbance term $\xi_{\text{GHG (anthr)}}^{S}$. Thus, we may say that the effect of anthropogenic global-scaled changes is not detected at all in the simulated annual mean temperature in the Arctic during 850–1849 AD. In our opinion, this conclusion is somewhat surprising, albeit the effect of anthropogenic changes may have been detected if the analysis period had extended longer after 1849 AD.

Concerning the external natural forcings, namely the solar, orbital and volcanic forcings, the estimates in Table S1.2.4 indicate that their (direct) effects are detected in the simulated annual mean temperature in the Arctic during 850–1849 AD. For example, for data set no. 5, $\widehat{Ssim} = 0.091$ with p value$= 5.5e$–06, $\widehat{Osim} = 0.082$ with p value$= 1.5e$–04, and $\widehat{Vsim} = 0.211$ with p value$= 9.9e$–23.

S1.2.5   Summary and conclusion (region: the Arctic)

The first statistical model, the ME-CFA(6, 5) model, is rejected due to inadmissble solutions.

It is also difficult to accept the modified CFA(7, 6) model due to its poor fit to the data.

In contrast, the SEM model demonstrated a much better fit to the data, which could be accepted both statistically and heuristically. In addition, the solutions observed were admissible for each data set analysed. Importantly, the interpretation of the SEM model, suggested quite a complex underlying data structure, seems to be reasonable from the climatological points of view for the period under consideration. Therefore, our suggestion is to choose the SEM model as a statistically adequate and climatologically defensible approximation of the underlying latent structure of the Arctic data.

S1.3 Asia (summer, June-August, mean temperature)

The data analysed are presented in Table S1.3.1, from which it follows that 10 data sets were analysed. Results for the three statistical models of interest are provided in Tables S1.3.2 - S1.3.4.

Table S1.3.1. Overview of replicates of each x_{f}, used to construct 10 regional Asia data sets. Each data set contains different $\bar{x}_{\mathrm{comb}}$ and τ_{pseudo}, where $\bar{x}_{\mathrm{comb}}$ is constructed by averaging over five replicates randomly selected from the nine that remained after one of $x_{\mathrm{comb\,repl}.i}$:s, $i = 1, \ldots, 10$, is chosen to represent τ, i.e. τ_{pseudo}.

			Mean sequences				
Data set	x_{Sol}	x_{Orb}	x_{Volc}	$x_{\mathrm{Land\,(anthr)}}$	x_{GHG}	x_{comb}	$x_{\mathrm{comb\,repl}.i} = \tau_{\mathrm{pseudo}}$
1	1,2,3	2,3	all associated repl's	1,2	2, 3	$(2,3,6,7,9)$	1
2	1,2,3	2,3	all associated repl's	1,2	2, 3	$(3,4,5,8,9)$	2
3	1,2,3	2,3	all associated repl's	1,2	2, 3	$(1,2,5,6,7)$	3
4	1,2,3	2,3	all associated repl's	1,2	2, 3	$(1,3,6,7,9)$	4
5	1,2,3	2,3	all associated repl's	1,2	2, 3	$(1,3,6,8,10)$	5
6	1,2,3	2,3	all associated repl's	1,2	2, 3	$(1,4,5,8,9)$	6
7	1,2,3	2,3	all associated repl's	1,2	2, 3	$(1,3,4,6,10)$	7
8	1,2,3	2,3	all associated repl's	1,2	2, 3	$(2,3,4,5,7)$	8
9	1,2,3	2,3	all associated repl's	1,2	2, 3	$(1,2,4,6,7)$	9
10	1,2,3	2,3	all associated repl's	1,2	2, 3	$(1,3,5,6,8)$	10

S1.3.1 Preliminary analyses of final single-forcing ensembles by means of the CFA(k_{f}, 1) model

The analysis of the the x_{Orb}- and x_{Volc} ensembles by means of the CFA($k_{\mathrm{f}}, 1$) model indicated that the effects of these forcings may be well detected in the simulated summer JJA mean temperature in Asia during $850-1849$ AD. The associated coefficients were estimated to be $\widehat{\alpha}_{\mathrm{Orb}} = 0.036$ with p value$= 1.9e{-}04$, $\widehat{\alpha}_{\mathrm{Volc}} = 0.202$ with p value$= 1.3e{-}38$. The analysis of the $x_{\mathrm{Land\,(anthr)}}$ ensemble also revealed a strong systematic signal in the simulated data ($\widehat{\alpha}_{\mathrm{Land\,(anthr)}} = 0.047$ with p value$= 6.1e{-}08$). Under our assumption that the (systematic) effect of the seasonal and interannual changes in the vegetation phenology on the temperature is negligible regardless the region, the strong signal observed is to be attributed to the antropogenic land-use forcing.

In contrast to the volcanic, orbital and land-use forcings, the effect of the solar forcing was not detected in the temperature generated by the x_{Sol} climate model ($\widehat{\alpha}_{\mathrm{Sol}} = 0.012$ with p value$= 0.5$). Finally, the analysis of the x_{GHG} ensemble indicated that the effect of the GHG forcing is weak, rather than strong ($\widehat{\alpha}_{\mathrm{GHG}} = 0.025$ with p value$= 0.06$).

S1.3.2 The result of fitting the ME-CFA(6, 5) model to the Asia data

As follows from Table S1.3.2, the ME-CFA(6, 5) model should be rejected as an adequate description of the underlying latent relationships. For two of 10 datasets, no solution could be observed. For the remaining eight data sets, the solutions were inadmissble. This is illustrated by the example of data set no. 1, for which the estimates of the three correlation coefficients, relating ξ_{Sol}^{S} to ξ_{Orb}^{S}, ξ_{Volc}^{S} and $\xi_{\mathrm{Land\,(anthr)}}^{S}$, respectively, have inadmissible values, that is, they are larger than 1 in absolute value.

18

Table S1.3.2. The result of estimating the ME-CFA(6, 5) model fitted to the Asia data. The estimates marked in bold font are inadmissble.

• *The result for data set no. 1*

Parameter	Estimate	p value	Parameter	Estimate	p value	Parameter	Estimate	p value
Ssim	0.001	5.4e–01	*Lsim*	0.047	3.6e–10	ϕ_{SG}	0.43	0.71
Strue	-0.039	6.6e–01	*Ltrue*	0.148	0.21	ϕ_{OV}	0.11	0.53
Osim	0.038	1.2e–06	*Gsim*	0.023	0.18	ϕ_{OL}	0.61	0.01
Otrue	-0.034	0.73	*Gtrue*	0.114	0.08	ϕ_{OG}	0.21	0.63
Vsim	0.119	1.3e–38	ϕ_{SO}	**1.32**	0.54	ϕ_{VL}	0.13	0.41
Vtrue	0.091	6.3e–02	ϕ_{SV}	**1.07**	0.52	ϕ_{VG}	0.51	0.08
			ϕ_{SL}	**1.98**	0.51	ϕ_{LG}	0.05	0.88

To assess the overall model fit:

Model $\chi^2 = 0.16$, df $= 1$, p value $= 0.69$, GFI $= 1.00$, AGFI $= 0.99$, SRMR $= 0.008$.

A similar result was observed for each data set except Data sets no. 2 and 7, for which the estimation procedure failed to converge to a solution.

S1.3.3 The result of fitting the CFA(7, 6) model to the Asia data

The insignificant estimate of α_{Sol} motivated us to estimate any version of the basic CFA model under the restriction *Ssim* $= 0$. This made it possible to avoid the effects of the empirical underidifiability, observed in the case of the ME-CFA(6, 5) model, and aided to gain additional degrees of freedom[1]. Setting *Ssim* to zero implies that $x_{\mathrm{Sol}} = \tilde{\delta}_{\mathrm{Sol}}$, that is, x_{Sol} represents the internal temperature variability generated by the x_{Sol}-climate model.

The numerical results for the final version of the CFA(7, 6) model, demonstrated the best fit to the data and the most stable performance, are given in Table S1.3.3. Examining the table, we first of all note that the resulting CFA model fits the data very well both according to the χ^2-statistic and to the heuristic indices. Importantly, this conclusion can be drawn across all data sets analysed.

Further, the resulting CFA model suggests that the (direct) effects of the orbital, volcanic, land-use and Ghg forcings are very well pronounced in the simulated summer JJA mean temperature in Asia during $850-1849$ AD. Once again, the effect of the volcanic forcing is estimated as the strongest. To see it, compare the estimates of *Osim*, *Vsim*, *Lsim* and *Gsim* to each other. For example, for data set no. 1, it was observed: $\widehat{Osim}$=0.025 (p value= 5.4e–05), $\widehat{Vsim}$=0.117 (p value= 1.2e–39), $\widehat{Lsim} = 0.050$, p value= 5.7e–18, and $\widehat{Gsim} = 0.032$, p value= 1.7e–07. These results seem to be supported by the temporal evolutions of the corresponding forcings, shown in Figures S4.2-S4.5 in Fetisova et al. (2017).

In the case of the GHG forcing, two aspects should be highlighted. The first one is that the CFA model also detected a weak correlation between ξ_{GHG}^S and ξ_{Volc}^S. Together with the significant estimate of *Gsim*, this result within our framework indicates that the significant effect of global-scale variations in the GHG forcing, detected by the CFA model in the simulated summer

---

[1]Here, we would like to emphasise that even if the effect of the solar forcing was expected to be strong, we would still set the correlation between ξ_{Sol}^S and $\xi_{\mathrm{Land\,(anthr)}}^S$ to zero. This is because within our framework anthropogenic forcings are not related to the natural ones, which implies the uncorrelatedness between accosiated temperature responses.

Table S1.3.3. The results of estimating the modified version of the CFA(7, 6) model fitted to the Asia data.

• *The result for data set no. 1*

Parameter	Estimate	p value	Parameter	Estimate	p value	Parameter	Estimate	p value
$Osim$	0.025	5.4e–05	$\sigma^2_{\eta_{\text{internal pseudo}}}$	0.007	2.9e–10	$\sigma_{\tilde\delta_{\text{Land (anthr)}}\,\tilde\delta_{\text{Sol}}}$	0.0008	0.014
$Vsim$	0.117	1.2e–39	ϕ_{VG}	0.30	0.08	$\sigma_{\tilde\delta_{\text{Land (anthr)}}\,\tilde\delta_{\text{Orb}}}$	0.2052	0.010
$Lsim$	0.050	5.7e–18	$\sigma_{\tilde\delta_{\text{Sol}}\,\tilde\delta_{\text{comb}}}$	0.0027	6.7e–06	$\sigma_{\tilde\delta_{\text{Sol}}\,\tilde\delta_{\text{Volc}}}$	0.0014	0.013
$Gsim$	0.032	1.0e–07	$\sigma_{\tilde\delta_{\text{Sol}}\,\eta_{\text{internal pseudo}}}$	0.0035	9.1e–08			

To assess the overall model fit:

Model $\chi^2 = 14.42$, df $= 17$, p value $= 0.64$, GFI $= 0.96$, AGFI $= 0.94$, SRMR $= 0.060$.

• *Summary of the results for all 10 data sets*

	Min	Mean	Max		Min	Mean	Max		Min	Mean	Max
$\widehat{Osim}$	0.021	0.025	0.027	$\widehat\sigma_{\tilde\delta_{\text{Sol}}\,\tilde\delta_{\text{comb}}}$	0.0026	0.0028	0.0030	Model χ^2	10.6	13.2	18.7
$\widehat{Vsim}$	0.117	0.117	0.118	$\widehat\sigma_{\tilde\delta_{\text{Sol}}\,\eta_{\text{internal pseudo}}}$	0.0025	0.0028	0.0035	p value	0.34	0.71	0.88
$\widehat{Lsim}$	0.047	0.049	0.051	$\widehat\sigma_{\tilde\delta_{\text{Land (anthr)}}\,\tilde\delta_{\text{Sol}}}$	7.2e–04	8.0e–04	8.4e–04	GFI	0.95	0.96	0.97
$\widehat{Gsim}$	0.032	0.033	0.035	$\widehat\sigma_{\tilde\delta_{\text{Land (anthr)}}\,\tilde\delta_{\text{Orb}}}$	0.205	0.208	0.212	AGFI	0.92	0.94	0.95
$\sigma^2_{\eta_{\text{internal pseudo}}}$	0.005	0.006	0.007	$\widehat\sigma_{\tilde\delta_{\text{Sol}}\,\tilde\delta_{\text{Volc}}}$	0.0013	0.0013	0.0014	SRMR	0.058	0.061	0.064
$\widehat\phi_{VG}$	0.277	0.297	0.326								

The solution for each data set is admissible.

340   JJA mean temperature in Asia during 850–1849 AD, is mostly of anthropogenic character. Climatologically, the significant effect of anthropogenic changes in GHG forcing can be justified by an effect in the last about one century of data in the analysed period.

     Another aspect is that the significant estimate of Gsim is not supported by the results of estimating the CFA($k_{\text{GHG}} = 2$, 1) model, which did not detect a strong systematic signal in the members of the x_{GHG} ensemble. This discrepancy in the

345 conclusions makes the highly significant estimate of *Gsim* dubious. In addition, it gives rise to a question as to what conclusion can be drawn if ξ^S_{GHG} is modelled as an endogenous variable in a SEM model, receiving causal inputs from other model variables. The SEM specification allows one to relate an endogenous latent variable to other model variables even if the variance of this endogenous variable, calculated afterwards, is expected to be weak, rather than strong. In other words, insignificant variability of an endogenous variable does not lead to the underidentifiability of the SEM model under consideration.

350 ### S1.3.4   The result of fitting the SEM model to the Asia data

The path diagram of the resulting SEM model is depicted in Fig. S1.3.1. As one can see, the SEM model, just as the CFA model above, also hypothesises that the solar forcing has a negligible effect on the simulated summer mean temperature in Asia during 850–1849 AD. That is, x_{Sol} represents the internal temperature variability generated by the x_{Sol}-climate model, denoted $\tilde\delta_{\text{Sol}}$.

355   The absence of ξ_{Sol}^S makes it possible to relate $\tilde{\delta}_{\text{Sol}}$ to other model variables through regressions instead of covariances, as it was done under the above presented CFA model. To be able to implement the desired causal relationships without changing the interpretation of x_{Sol}, a new observable variable, denoted x_{Sol}^+, was constructed. The construction principles were the same as those used for constructing the variable $x_{\text{Land (anthr)}}^+$ in the SEM model applied to the Europe data (for the details, see Sect. S1.1. and Fig. S1.1.1).
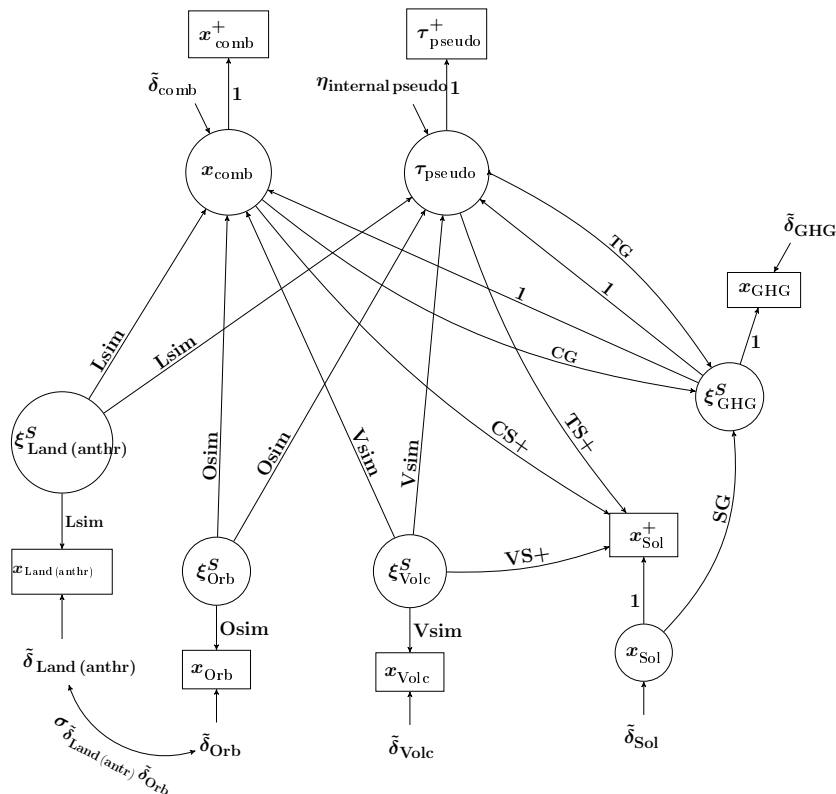
Figure S1.3.1. Path diagram of the SEM model fitted to the Asia data.

360

As follows from Fig. S1.3.1, x_{Sol}^+ receives the three causal inputs from x_{comb}, τ_{pseudo} and ξ_{Volc}^S, respectively. Hence, the SEM model relates $\tilde{\delta}_{\text{Sol}}$ to all forced components, included in the SEM model, and to the internal variability generated by the multi-forcing climate model. In the real-world climate system, these relationships could be explained by interactions between the internal processes and the climate system, which may be reflected in the forcing reconstructions and the physical basis for describing the internal processes in the climate model under consideration.

365   Further, the SEM model suggests complex reciprocal relationships between ξ_{GHG}^S and some other model variables, including all the forced components. As one can see, ξ_{GHG}^S receives three causal inputs from x_{comb}, τ_{pseudo} and x_{Sol}, respectively (see the paths *CG*, *TG*, and *SG*). In the real-world climate system, the counterpart of these relationships can be reciprocal interactions between the climate system and the concentrations of the greenhouse gases in the atmosphere.

Table S1.3.4. The result of fitting the SEM model depicted in Fig. S1.3.1 (region: Asia).

● *The result for data set no. 1*

Parameter	Estimate	p value	Parameter	Estimate	p value	Parameter	Estimate	p value
$Osim$	0.032	$6.8e\text{--}09$	$CS+$	0.303	0.003	CG	-0.042	0.47
$Vsim$	0.117	$1.6e\text{--}39$	$TS+$	0.119	0.033	TG	0.125	0.012
$Lsim$	0.047	$5.7e\text{--}18$	$VS+$	-0.042	0.001	SG	-0.028	0.004
$\sigma^2_{\eta_\text{internal pseudo}}$	0.007	$6.0e\text{--}10$	$\sigma_{\tilde{\delta}_\text{Land (anthr)}\,\tilde{\delta}_\text{Orb}}$	0.001	0.023			

$$\sqrt{\widehat{\mathrm{Var}}(\xi^S_\text{GHG})} = \widehat{Gsim}_{SEM} = \sqrt{\left(\left(\widehat{Lsim}\cdot(\widehat{CG}+\widehat{TG})\right)^2 + \left(\widehat{Osim}\cdot(\widehat{CG}+\widehat{TG})\right)^2 + \left(\widehat{Vsim}\cdot(\widehat{CG}+\widehat{TG})\right)^2\right) \Big/ \left(\widehat{CG}+\widehat{TG}-1\right)^2 +}$$

$$\overline{+ \left(\widehat{SG}^2\cdot\sigma^{2\,*}_{\tilde{\delta}_\text{Sol}} + \widehat{CG}^2\cdot\sigma^{2\,*}_{\tilde{\delta}_\text{comb}} + \widehat{TG}^2\cdot\widehat{\sigma}^2_{\eta_\text{internal pseudo}}\right) \Big/ \left(\widehat{CG}+\widehat{TG}-1\right)^2} = 0.022 \quad (p\,\text{value} = 0.020)$$

To assess the overall model fit:

$$\text{Model } \chi^2 = 10.20, \quad df = 17, \quad p\,\text{value} = 0.90, \quad GFI = 0.97, \quad AGFI = 0.96 \quad SRMR = 0.057.$$

● *Summary of the results for all 10 data sets*

	Min	Mean	Max		Min	Mean	Max		Min	Mean	Max
$\widehat{Osim}$	0.032	0.033	0.034	$\widehat{CS+}$	0.303	0.360	0.424	Model χ^2	10.2	12.60	19.20
$\widehat{Vsim}$	0.117	0.117	0.117	$\widehat{TS+}$	0.026	0.075	0.119	p value	0.32	0.75	0.90
$\widehat{Lsim}$	0.045	0.047	0.049	$\widehat{VS+}$	-0.047	-0.044	-0.042	GFI	0.95	0.97	0.97
$\widehat{CG}$	-0.042	0.083	0.202	$\widehat{\sigma}_{\tilde{\delta}_\text{Land (anthr)}\,\tilde{\delta}_\text{Orb}}$	0.001	0.001	0.001	AGFI	0.92	0.95	0.96
$\widehat{TG}$	-0.111	0.007	0.125	$\widehat{\sigma}^2_{\eta_\text{internal pseudo}}$	0.005	0.006	0.007	SRMR	0.056	0.058	0.062
$\widehat{SG}$	-0.111	-0.272	-0.254	$\widehat{Gsim}_{SEM}$	0.020	0.021	0.022				

The solution for each data set is admissible.

Unlike the CFA model above, the SEM model suggests that the overall (direct) effect of the GHG forcing is not strongly pronounced in the simulated summer (JJA) mean temperature in Asia during 850–1849 AD. This conclusion is based on the moderately significant estimate of the parameter $Gsim_{SEM}$ (see Table S1.3.4). For example, for Data set no. 1, for which the SEM model was initially formulated, the estimate of $\widehat{Gsim}_{SEM}$ is 0.022 with the associated p value of 0.020. Notice that this conclusion is in concert with the conclusion provided by the $\text{CFA}(k_\text{GHG}, 1)$ model.

Concerning the character of the GHG forcing, the SEM model describes it mostly as natural. Indeed, most of the inputs, received by ξ^S_GHG directly or indirectly, represent the effects of either the natural forcings or the internal processes. However, despite the fact that the disturbance term $\xi^S_\text{GHG (anthr)}$ is not in the SEM model, the anthropogenic impact can still be traced through the indirect influence from $\xi^S_\text{Land (anthr)}$.

The estimates of the *Osim* and *Vsim* indicate that the (direct) effects of the orbital respective volcanic forcings are well detected in the simulated summer (JJA) mean temperature in Asia during 850–1849 AD. For example, for data set no. 1, $\widehat{Osim}$ is 0.024 with the associated p value of $1.0e\text{--}04$, and $\widehat{Vsim}$ is 0.117 with p value of $1.2e\text{--}39$. Hence, just as in the previously

analysed regional data, we are once again observing that the volcanic forcing exhibits the strongest impact on the simulated temperature.

Even the (direct) effect of the anthropogenic land-use forcing is estimated as significant both for data set no. 1 and on
385　average. For data set no. 1, $\widehat{Lsim}$ is estimated to be 0.048 with the associated p value= $1.7e{-}17$.

The statistical and heuristical measures of the overall model fit, given in Table S1.3.4, assess the overall model fit as very good both for data set no. 1 and on average. For example, the χ^2 statistic for data set no. 1 is 10.20 with the p value of 0.90, which is much larger than 0.05, and the SRMR value is 0.057, which is less than 0.08.

S1.3.5　Summary and conclusion (region: Asia)

390　The first statistical model, the ME-CFA(6, 5) model, is rejected due to inadmissble solutions.

Both modified CFA(7, 6)- and SEM models demonstrated a very good overall fit to the data. Importantly, they fit to the data to a similar degree both statistically and heuristically. Compare, for example, the range of the χ^2 statistic, observed under the CFA model (min(χ^2)=10.6, mean(χ^2)=13.2, max(χ^2)=18.7), to the corresponding range, obtained under the SEM model (min(χ^2)=10.2, mean(χ^2) = 12.60, max(χ^2) = 19.20). One can also compare the ranges of the SRMR val-
395　ues: (min(SRMR)= 0.058, mean(SRMR)= 0.061, max(SRMR)= 0.064), associated with the CFA model, and (min(SRMR)= 0.056, mean(SRMR)= 0.058, max(SRMR)= 0.062), associated with the SEM model.

Moreover, both models demonstrated a stable performance across all data sets, and they lead the same conclusions about the direct effects of all the forcings except the GHG forcing. The CFA model suggested that the overall direct global-scaled effect of the GHG forcing is well pronounced in the simulated summer (JJA) mean temperature in Asia during $850-1849$
400　AD. In addition, the CFA model suggested that the nderlying forcing is of anthropogenic character. The SEM model, in contrast, described the GHG forcing as a natural forcing and its effect is moderately seen in the simulated summer (JJA) mean temperature in Asia during $850-1849$ AD. Both interpretations seem to be defensible from the climatological point of view. However, the conclusion, provided by the SEM model, is in concert with the conclusion provided by the CFA($k_{\text{GHG}} = 2, 1$) model, which did not detected a strong systematic signal in the temperature data generated by the x_{GHG} climate model. In our
405　opinion, this speaks in favour of the SEM model.

Therefore, our suggestion is to choose the SEM model as a more statistically reliable description of the unknown underlying structure of the Asia data, compared to the CFA model.

S1.4 South America (summer, December-February (DJF), mean temperature)

The data sets analysed are presented in Table S1.4.1, from which it follows that seven data sets were analysed. Results for the three statistical models of interest are provided in Tables S1.4.2 - S1.4.3.

Table S1.4.1. Overview of replicates of each x_{f}, used to construct seven regional South America data sets. Each data set contains different $\bar{x}_{\mathrm{comb}}$ and τ_{pseudo}, where $\bar{x}_{\mathrm{comb}}$ is constructed by averaging over three replicates randomly selected from the six that remained after $x_{\mathrm{comb\,repl.}}$:s, $i = 1, 3, 5$, have been eliminated and after one of $x_{\mathrm{comb\,repl.}i}$:s, $i = 2, 4, 6, 7, 8, 9, 10$, is chosen to represent τ, i.e. τ_{pseudo}.

Data set	x_{Sol}	x_{Orb}	x_{Volc}	$x_{\mathrm{Land\,(anthr)}}$, x_{GHG}	x_{comb}	$\tau_{\mathrm{pseudo}} = x_{\mathrm{comb\,repl.}i}$
				Mean sequences		
1	2,3,4	1,3	3,5	all associated repl's	$(4, 6, 10)$	2
2	2,3,4	1,3	3,5	all associated repl's	$(7, 8, 10)$	4
3	2,3,4	1,3	3,5	all associated repl's	$(7, 8, 9)$	6
4	2,3,4	1,3	3,5	all associated repl's	$(6, 9, 10)$	7
5	2,3,4	1,3	3,5	all associated repl's	$(6, 7, 9)$	8
6	2,3,4	1,3	3,5	all associated repl's	$(2, 7, 8)$	9
7	2,3,4	1,3	3,5	all associated repl's	$(2, 4, 6)$	10

S1.4.1 Preliminary analyses of final single-forcing ensembles by means of the CFA(k_{f}, 1) model

As a preliminary step, each of the single-forcing ensemble in Table S1.4.1 was analysed by means of the CFA(k_{f}, 1) model. The results indicated that the effect of the orbital and volcanic forcings on the simulated summer (DJF) mean temperature in South America during 850–1849 AD may be strong ($\widehat{\alpha}_{\mathrm{Orb}} = 0.086$ with p value $= 1.410e{-}11$, $\widehat{\alpha}_{\mathrm{Volc}} = 0.108$ with p value $= 5.001e{-}18$).

In contrast, no systematic effect of the solar forcing was detected in the temperature sequences, generated by the x_{Sol}-climate model ($\widehat{\alpha}_{\mathrm{Sol}} = 0.009$, p value $= 0.824$). The same conclusion was drawn for the land-use and GHG forcings, whose estimated effects were given by $\widehat{\alpha}_{\mathrm{Land\,(anthr)}} = 2.830e{-}06$ with p value $= 1.00$ and $\widehat{\alpha}_{\mathrm{GHG}} = 0.024$ with p value $= 0.25$, respectively.

In the case of the solar and land-use forcings, the conclusion of a non-detectable effect was also supported by the fact that the a priori obtained estimates of $\sigma^{2\,*}_{\bar{\delta}_{\mathrm{Sol}}}$ and $\sigma^{2\,*}_{\bar{\delta}_{\mathrm{Land\,(anthr)}}}$ turned out to be larger than the sample variance of the corresponding observed mean-sequences. Therefore, in each statistical model analysed, $\sigma^{2\,*}_{\bar{\delta}_{\mathrm{f}}}$, $\mathrm{f} \in \{\mathrm{Sol, Land\,(anthr)}\}$, was set to the sample variance of the corresponding x_{f} mean sequence. Statistically, it implies that x_{f} does not contain the forced component ξ^{S}_{f}.

S1.4.2 The result of fitting the ME-CFA(6, 5) model to the South America data

Given the preliminary estimates of α_{f}:s, it is expected that the estimation of the ME-CFA(6, 5) model, treating *Ssim*, *Lsim*, *Gsim* and all associated correlation coefficients as free parameters, does not work. As we can see in Table S1.4.2, this is the case. To begin with, the solution could be observed only for one data set (data set no. 7), while for the remaining seven data sets the estimation procedure failed to converge to a solution. Further, for data set no. 7, the estimates of the three correlation coefficients, associated with the simulated temperature responses to the solar, land use and GHG forcings, turned out to be

24

inadmissble (each of them is larger than 1 in absolute value). Thus, the ME-CFA(6, 5) model has to be rejected, regardless of its fit to the data.

Table S1.4.2. The result of estimating the ME-CFA(6, 5) model fitted to the South America data. The estimates marked in bold font are inadmissble.

● *The result for data set no. 7*

Parameter	Estimate	p value	Parameter	Estimate	p value	Parameter	Estimate	p value
Ssim	0.011	0.74	*Lsim*	0.017	0.41	ϕ_{SG}	**-2.67**	0.74
Strue	0.018	0.77	*Ltrue*	-0.042	0.61	ϕ_{OV}	-0.19	0.23
Osim	0.081	6.8e–14	*Gsim*	-0.026	0.12	ϕ_{OL}	0.42	0.55
Otrue	0.068	0.27	*Gtrue*	-0.017	0.73	ϕ_{OG}	0.01	0.97
Vsim	0.108	2.9e–20	ϕ_{SO}	0.50	0.77	ϕ_{VL}	0.09	0.86
Vtrue	0.085	0.09	ϕ_{SV}	**1.91**	0.73	ϕ_{VG}	0.19	0.61
			ϕ_{SL}	**1.99**	0.74	ϕ_{LG}	-0.12	0.93

To assess the overall model fit:

Model $\chi^2 = 0.86$, df $= 1$, p value $= 0.35$, GFI $= 0.99$, AGFI $= 0.94$, SRMR $= 0.019$.

For the remaining six data sets, the estimation algorithm failed to converge to a solution.

S1.4.3 The result of fitting the CFA(7, 6) model to the South America data

In order to avoid inadmissible solutions and gain as many degrees of freedom as possible, all versions of the basic CFA(7, 6) model were estimated under the restrictions that *Ssim*, *Lsim*, *Gsim* and all correlation coefficients, associated with ξ_{Sol}^S, $\xi_{\text{Land (anthr)}}^S$, and ξ_{GHG}^S, are zero. This corresponds to hypothesising that the effects of the solar, land-use and GHG forcings are not detectable in the simulated summer (DJF) mean temperature in South America during 850–1849 AD.

According to the numerical results, presented in Table S1.4.3, we may conclude that the overall fit of the presented CFA model is reasonably good both statistically and heuristically. For example, for data set no. 1, the p value for the χ^2 statistic, 0.73, is larger than 0.05. The heuristic indices GFI and AGFI, 0.96 and 0.94, respectively, are both larger than the recommended cutoff values of 0.9 and 0.8, respectively. Finally, the SRMR value of 0.073 is smaller than the associated cutoff value of 0.08. A certain impairment of the model fit was observed for data set no. 6, which was indicated by quite a high SRMR value (SRMR$= 0.087 > 0.08$). The analysis of the residual matrix suggested that the impairment of the fit could be due to a significant correlation between $\tilde{\delta}_{\text{GHG}}$ and $\eta_{\text{internal pseudo}}$. However, since this correlation was far away from being significant for the remaining six data sets, it was decided not to estimate it for all data sets.

The estimates of Osim and Vsim suggest that the (direct) effects of the orbital and volcanic forcings are well detected in the simulated summer (DJF) mean temperature in South America during 850–1849 AD. For example, for data set no. 1, $\widehat{Osim}$ is 0.070 with the associated p value of 9.6e–17, and $\widehat{Vsim}$ is 0.108 with the associated p value of 7.9e–28. Comparing the estimates of *Osim* and *Vsim*, we once again can conclude that the effect of the volcanic forcing is estimated as the largest one.

Table S1.4.3. The result of estimating the modified version of the CFA(7, 6) model fitted to the South America data.

● *The result for data set no. 1*

Parameter	Estimate	p value	Parameter	Estimate	p value	Parameter	Estimate	p value
$Osim$	0.070	9.6e–17	$\sigma_{\tilde{\delta}_{\text{Land (anthr)}}\,\tilde{\delta}_{\text{comb}}}$	0.0013	0.08	$\sigma_{\tilde{\delta}_{\text{Sol}}\,\tilde{\delta}_{\text{comb}}}$	0.0019	0.043
$Vsim$	0.108	7.9e–28	$\sigma_{\tilde{\delta}_{\text{Land (anthr)}}\,\eta_{\text{internal pseudo}}}$	0.0010	0.32	$\sigma_{\tilde{\delta}_{\text{Sol}}\,\eta_{\text{internal pseudo}}}$	0.0019	0.11
$\sigma^2_{\eta_{\text{internal pseudo}}}$	0.015	3.3e–09	$\sigma_{\tilde{\delta}_{\text{Orb}}\,\tilde{\delta}_{\text{comb}}}$	-0.0011	0.34			
$\sigma_{\tilde{\delta}_{\text{Sol}}\,\tilde{\delta}_{\text{Volc}}}$	0.024	0.001	$\sigma_{\tilde{\delta}_{\text{Orb}}\,\eta_{\text{internal pseudo}}}$	-0.0036	0.031			

To assess the overall model fit:

Model $\chi^2 = 14$, df $= 18$, p value $= 0.73$, GFI $= 0.96$, AGFI $= 0.94$, SRMR $= 0.073$.

● *Summary of the results for all 7 data sets*

	Min	Mean	Max		Min	Mean	Max		Min	Mean	Max
$\widehat{Osim}$	0.070	0.071	0.073	$\widehat{\sigma}_{\tilde{\delta}_{\text{Orb}}\,\tilde{\delta}_{\text{comb}}}$	-0.0036	-0.0016	0.00	Model χ^2	10.0	15.0	19.5
$\widehat{Vsim}$	0.105	0.107	0.108	$\widehat{\sigma}_{\tilde{\delta}_{\text{Orb}}\,\eta_{\text{internal pseudo}}}$	-0.0028	-0.0018	-0.0011	$p$value	0.36	0.66	0.85
$\widehat{\sigma}^2_{\eta_{\text{internal pseudo}}}$	0.013	0.016	0.019	$\widehat{\sigma}_{\tilde{\delta}_{\text{Sol}}\,\tilde{\delta}_{\text{Volc}}}$	0.0021	0.0022	0.0022	GFI	0.95	0.96	0.97
$\widehat{\sigma}_{\tilde{\delta}_{\text{Sol}}\,\tilde{\delta}_{\text{comb}}}$	0.0018	0.0020	0.0021	$\widehat{\sigma}_{\tilde{\delta}_{\text{Land (anthr)}}\,\tilde{\delta}_{\text{comb}}}$	8.0e–05	0.0011	0.0017	AGFI	0.92	0.94	0.95
$\widehat{\sigma}_{\tilde{\delta}_{\text{Sol}}\,\eta_{\text{internal pseudo}}}$	0.0016	0.0020	0.0028	$\widehat{\sigma}_{\tilde{\delta}_{\text{Land (anthr)}}\,\eta_{\text{internal pseudo}}}$	-1.0e–04	0.0013	0.0042	SRMR	0.068	0.073	0.087

The solution for each data set is admissible.

Let us also point out the fact that in order to achieve an acceptable model fit of the CFA model to the data it was necessary to free up several specific factor covariances, five of which are related to x_{Sol} and $x_{\text{Land (anthr)}}$. Since these variables do not contain forced components, this gave rise to a question as to whether the covariances between the corresponding observable variables
450 can be modelled by means of regressions. To this end, the underlying structure of the data was analysed by means of the SEM model. The result is described below.

S1.4.4 The result of fitting the SEM model to the South America data

The path diagram of the resulting SEM model is shown in Fig. S1.4.1. This SEM model demonstrated the best fit to the data and the most stable performance among different versions of the basic SEM model. As one can see in Fig. S1.4.1, the SEM
455 model, just as the CFA model above, hypothesises that the direct effects of the solar, land-use and GHG forcings are not detectable. That is, x_{Sol}, $x_{\text{Land (anthr)}}$ and x_{GHG} contain only the internal temperature variability, generated by the corresponding single-forcing climate model, i.e. $x_{\text{Sol}} = \tilde{\delta}_{\text{Sol}}$, $x_{\text{Land (anthr)}} = \tilde{\delta}_{\text{Land (anthr)}}$ and $x_{\text{GHG}} = \tilde{\delta}_{\text{GHG}}$.

One can also see in Fig. S1.4.1, the SEM model contains two new observable variables, not presented even in the basic SEM model described in LAS22num. The variables are x^+_{Sol} and $x^+_{\text{Land (anthr)}}$, each of which was constructed in an analogous way and
460 for the same purpose as $x^+_{\text{Land (anthr)}}$ and x^+_{Orb} in the SEM model fitted to the Europe data (see Sect. S1.1 here).

Each of the new variables receives causal inputs from x_{comb} and τ_{pseudo}, denoted *CL+*, *TL+*, *CS+*, and *TS+*.
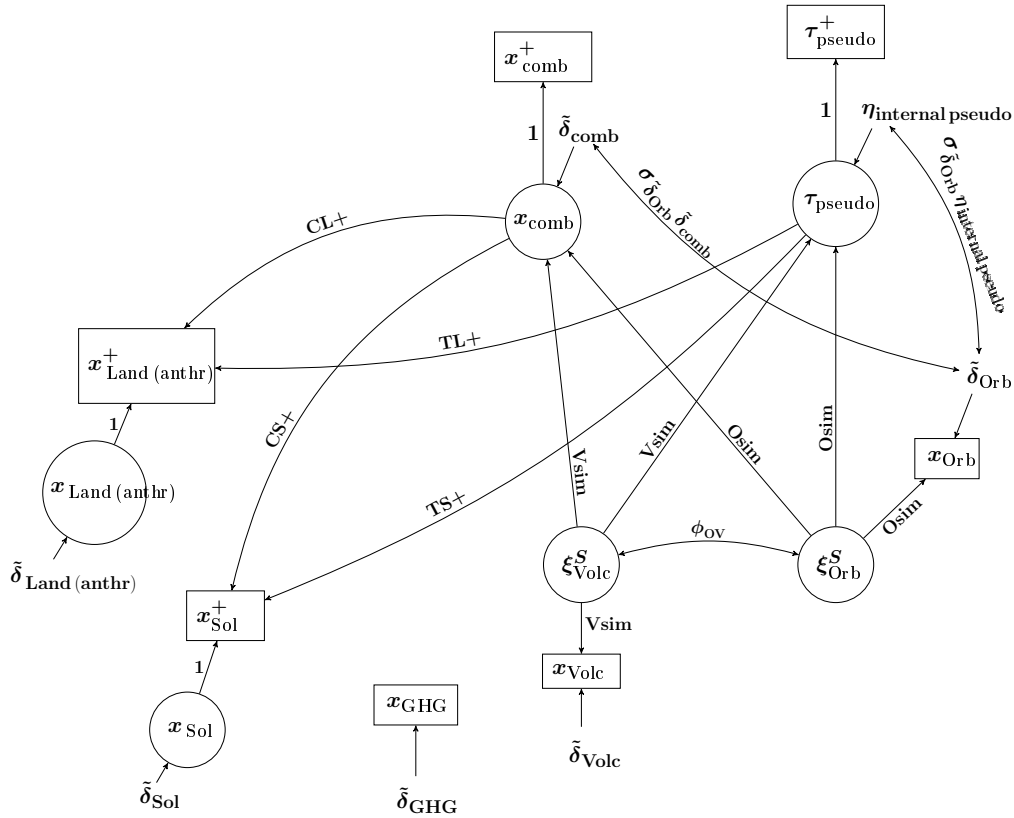
Figure S1.4.1. Path diagram of the SEM model fitted to the South America data.

Hence, the SEM model relates $\tilde{\delta}_{\text{Sol}}$ and $\tilde{\delta}_{\text{Land (anthr)}}$, represented by x^+_{Sol} and $x^+_{\text{Land (anthr)}}$, respectively, not only to $\tilde{\delta}_{\text{comb}}$ and $\eta_{\text{internal pseudo}}$ (as it was done under the CFA model by means of the specific-factor covariances), but also to the forced components ξ^S_{Volc} and ξ^S_{Orb}, embedded in x_{comb} and τ_{pseudo} (and in x_{Volc} and x_{Orb}, respectively).

465   In the real-world climate system, these co-relations could be explained by interactions, i.e. feedback mechanisms, between the internal processes and the climate system, in particular the volcanic and orbital forcing. Note that the estimates of these four parameters turned out to be statistically insignificant. For example, for data set no. 1, it was observed: $\widehat{CL+}$ =0.085 with p value 0.19, $\widehat{TL+} = -0.002$ with p value 0.97, $\widehat{CS+} = 0.104$ with p value 0.12, and $\widehat{TS+} = 0.018$ with p value= 0.74 (see Table S1.4.4).

470   Nevertheless, despite their statistical insignificance, it was crucial to free up these paths for achieving a better overall model fit, compared to the overall fit of the CFA model. The improvement is especially seen in the smaller residuals, expressed by the SRMR values. Compare the range of the SRMR values for the CFA model, (min(SRMR)= 0.068, mean(SRMR)= 0.073, max(SRMR)= 0.087), to the corresponding range observed under the SEM model, (min(SRMR)= 0.055, mean(SRMR)= 0.059, max(SRMR)= 0.071). Taking into consideration the fact that both statistical models have the same degrees of freedom,

475   i.e. they estimate the same no. of parameters, we may say that the decrease in the SRMR values under the SEM model is substantial, which speaks in favor of the SEM model.

Table S1.4.4. The result of fitting the SEM model depicted in Fig. S1.4.1 (region: South America).

• *The result for data set no. 1*

Parameter	Estimate	p value	Parameter	Estimate	p value
$Osim$	0.074	7.8e–17	$CS+$	0.104	0.12
$Vsim$	0.113	1.6e–26	$TS+$	0.018	0.74
$\sigma^2_{\eta_{\text{internal pseudo}}}$	0.015	2.9e–09	$\sigma_{\tilde{\delta}_{\text{Orb}}\,\tilde{\delta}_{\text{comb}}}$	-0.0007	0.55
$CL+$	0.085	0.19	$\sigma_{\tilde{\delta}_{\text{Orb}}\,\eta_{\text{internal pseudo}}}$	-0.0034	0.044
$TL+$	-0.002	0.97	ϕ_{OV}	-0.21	0.12

To assess the overall model fit:

Model $\chi^2 = 12.5$,   df $= 18$, p value $= 0.82$,   GFI $= 0.97$,   AGFI $= 0.95$,   SRMR $= 0.057$.

• *Summary of the results for all 7 data sets*

	Min	Mean	Max		Min	Mean	Max		Min	Mean	Max
$\widehat{Osim}$	0.072	0.074	0.076	$\widehat{CS+}$	0.062	0.093	0.119	Model χ^2	11.3	13.8	18.1
$\widehat{Vsim}$	0.111	0.112	0.113	$\widehat{TS+}$	0.002	0.029	0.068	p value	0.45	0.73	0.88
$\widehat{\sigma}^2_{\eta_{\text{internal pseudo}}}$	0.014	0.017	0.019	$\widehat{\sigma}_{\tilde{\delta}_{\text{Orb}}\,\tilde{\delta}_{\text{comb}}}$	-0.0023	-0.0014	0.0007	GFI	0.95	0.96	0.97
$\widehat{CL+}$	-0.038	0.056	0.151	$\widehat{\sigma}_{\tilde{\delta}_{\text{Orb}}\,\eta_{\text{internal pseudo}}}$	-0.0034	-0.0012	0.0007	AGFI	0.93	0.95	0.96
$\widehat{TL+}$	-0.066	0.023	0.148	$\widehat{\phi}_{OV}$	-0.227	-0.205	-0.189	SRMR	0.055	0.059	0.071

The solution for each data set is admissible

Other parameters, whose estimation contributed substantially to the improvement of the overall model fit, are the covariance between $\tilde{\delta}_{\text{Orb}}$ and $\tilde{\delta}_{\text{comb}}$ denoted $\sigma_{\tilde{\delta}_{\text{Orb}}\,\tilde{\delta}_{\text{comb}}}$, the covariance between $\tilde{\delta}_{\text{Orb}}$ and $\eta_{\text{internal pseudo}}$, denoted $\sigma_{\tilde{\delta}_{\text{Orb}}\,\eta_{\text{internal pseudo}}}$, and the correlation between ξ^S_{Volc} and ξ^S_{Orb}, denoted ϕ_{OV}. Just as the estimates of the above-discussed paths, the estimates of these

480   parameters turned out to be insignificant or slightly significant across all data sets. For example, for data set no. 1, it was observed: $\widehat{\sigma}_{\tilde{\delta}_{\text{Orb}}\,\tilde{\delta}_{\text{comb}}} = -0.0007$ with p value$= 0.55$, $\widehat{\sigma}_{\tilde{\delta}_{\text{Orb}}\,\eta_{\text{internal pseudo}}} = -0.0034$ with p value$=0.044$, and $\widehat{\phi}_{OV} = -0.21$ with p value$= 0.12$. An important note on the latter estimate is that its insignificance is in concert with our basic assumption that the temperature responses to the external natural forcings are mutually uncorrelated.

Just as the CFA model, the SEM model detects a well pronounced effects of the orbital and volcanic forcings in the simulated

485   summer (DJF) mean temperature in South America during $850-1849$ AD. Moreover, just as the CFA model, the SEM model also estimates the effect of the volcanic forcing as the strongest one. For example, for data set no. 1, the estimates obtained under the SEM model are: $\widehat{Osim} = 0.074$ with the associated p value of 7.8e–17, and $\widehat{Vsim} = 0.113$ with the associated p value of 1.6e–26.

S1.4.5   Summary and conclusions (region: South America)

The first statistical model, the ME-CFA(6, 5) model, is rejected due to inadmissble solutions.

Both CFA and SEM models have admissible solutions and an acceptable overall fit to the data. Importantly, both models lead to the same conclusions about the direct effects of forcings, namely that the effects of the volcanic and orbital forcings are well detected in the simulated summer (DJF) mean temperature in South America during $850-1849$ AD, while the effects of the solar, land-use and GHG forcings are not detected. This interpretation seems to be climatologically defensible for the region and period under study. Moreover, it is supported by the preliminary analyses of the single-forcing ensembles by means of the CFA$(k_f, 1)$ model, which increases our confidence in the conclusions drawn.

An advantage of the SEM model is that the SEM model fits the data better than the CFA model, especially in terms of the residuals, summarised by the SRMR values. Keeping in mind that both statistical models have the same number of degrees of freedom (df=18), the better overall fit of the SEM model motivates us to prefer the SEM model as a more adequate approximation of the underlying structure of the South America data.

S1.5   Australasia (warm-season, September-February, mean temperature)

The data sets analysed are presented in Table S1.5.1, from which it follows that nine data sets were analysed. Results for the three statistical models of interest are provided in Tables S1.5.2 - S1.5.4.

Table S1.5.1. Overview of replicates of each x_{f}, used to construct 9 regional Australasia data sets. Each data set contains different $\bar{x}_{\mathrm{comb}}$ and τ_{pseudo}, where $\bar{x}_{\mathrm{comb}}$ is constructed by averaging over five replicates randomly selected from the eight that remained after $x_{\mathrm{comb\,repl.4}}$ has been eliminated and after one of $x_{\mathrm{comb\,repl.}i}$:s, $i = 1,2,3,5,6,7,8,9,10$, is chosen to represent τ, i.e. τ_{pseudo}.

	Mean sequences						
Data set	x_{Sol}	x_{Orb}	x_{Volc},	$x_{\mathrm{Land\,(anthr)}}$	x_{GHG}	x_{comb}	$x_{\mathrm{comb\,repl.}i} = \tau_{\mathrm{pseudo}}$
1	2,3,4	all associated replicates	1,2,5	2,3	2,3	$(2,3,7,8,10)$	1
2	2,3,4	all associated replicates	1,2,5	2,3	2,3	$(3,5,6,9,10)$	2
3	2,3,4	all associated replicates	1,2,5	2,3	2,3	$(1,2,6,7,8)$	3
4	2,3,4	all associated replicates	1,2,5	2,3	2,3	$(1,3,7,8,10)$	5
5	2,3,4	all associated replicates	1,2,5	2,3	2,3	$(1,2,7,9,10)$	6
6	2,3,4	all associated replicates	1,2,5	2,3	2,3	$(1,5,6,9,10)$	7
7	2,3,4	all associated replicates	1,2,5	2,3	2,3	$(2,3,5,7,9)$	8
8	2,3,4	all associated replicates	1,2,5	2,3	2,3	$(2,3,4,6,8)$	9
9	2,3,4	all associated replicates	1,2,5	2,3	2,3	$(1,2,5,7,8)$	10

S1.5.1   Preliminary analyses of final single-forcing ensembles by means of the CFA(k_{f}, 1) model

505   The preliminary analysis of each single-forcing ensemble by means of the CFA(k_{f}, 1) model led to the following results:

- the effect of the solar forcing is moderately pronounced in the simulated Sep-Feb temperatures in Australasia during the period 850–1849 AD ($\widehat{\alpha}_{\mathrm{Sol}} = 0.017$ with p value= 0.020);

- the effect of the orbital forcing is weakly pronounced ($\widehat{\alpha}_{\mathrm{Orb}} = 0.015$ with p value= 0.047);

- the effect of the volcanic forcing is once again estimated as the strongest and the most significant among the effects of
510   the purely natural forcings ($\widehat{\alpha}_{\mathrm{Volc}} = 0.079$ with p value= $3.2e$–31);

- the effect of the anthropogenic land use forcing could not be detected at all in the Sep-Feb temperature generated by the $x_{\mathrm{Land\,(anthr)}}$ climate model ($\widehat{\alpha}_{\mathrm{Land\,(anthr)}} = 0.00015$ with p value= 0.99); This conclusion is in agreement with the reconstruction of the land-use forcing, shown in Fig. S4.5 in Fetisova et al. (2017);

- the effect of the GHG forcing was estimated as significant ($\widehat{\alpha}_{\mathrm{GHG}} = 0.033$ with p value= $1.4e$–04), although within the
515   CFA(k_{f}, 1) model it is not clear whether this effect is of anthropogenic, natural, or mixed character).

S1.5.2   The result of fitting the ME-CFA(6, 5) model to the Australasia data

As follows from Table S1.5.2, the estimation of the ME-CFA(6, 5) model resulted in inadmissible solutions for seven of nine data sets. For the remaining two data sets, no estimates could be obtained because the estimation procedure failed to converge to a solution. The estimates of the correlation coefficients, relating $\xi^S_{\text{Land (anthr)}}$ to other temperature responses, laid outside their admissible range between -1 and 1. Bearing in mind that the effect of the land-use forcing was described by the $\text{CFA}(k_\text{f}, 1)$ model as nondetectable and the effect of the orbital forcing is estimated as weak rather than strong, this result of estimating the ME-CFA(6, 5) model is quite expected.

Table S1.5.2. The result of estimating the ME-CFA(6, 5) model fitted to the Australasia data. The estimates marked in bold font are inadmissble

- *The result for data set no. 1*

Parameter	Estimate	p value	Parameter	Estimate	p value
Ssim	0.019	5.6e–04	ϕ_{SO}	0.28	0.62
Strue	0.034	0.26	ϕ_{SV}	0.14	0.53
Osim	0.014	0.06	ϕ_{SL}	**2.09**	0.48
Otrue	0.002	0.94	ϕ_{SG}	-0.36	0.31
Vsim	0.079	5.4e–31	ϕ_{OV}	0.20	0.53
Vtrue	0.074	1.3e–05	ϕ_{OL}	**2.58**	0.49
Lsim	0.010	0.49	ϕ_{OG}	0.04	0.94
Ltrue	0.012	0.59	ϕ_{VL}	0.31	0.64
Gsim	-0.033	3.3e–06	ϕ_{VG}	0.32	0.86
Gtrue	-0.012	0.65	ϕ_{LG}	-0.30	0.73

To assess the overall model fit:

$$\text{Model } \chi^2 = 0.092, \quad \text{df} = 1, \quad p \text{ value} = 0.76, \quad \text{GFI} = 1, \quad \text{AGFI} = 0.99, \quad \text{SRMR} = 0.005.$$

A similar result has been observed for all 9 data sets except Data sets no. 3 and 7, for which the estimation procedure failed to converge to a solution.

S1.5.3   The result of fitting the CFA(7, 6) model to the Australasia data

Among several versions of the CFA(7, 6) model considered, the most stable performance was demonstrated by the CFA model, presented in Table S1.5.3. Nevertheless, it should be added that the CFA model was sensitive to starting values for the covariances between the specific factors. Without freeing up these covariances, the model could be estimated for all data sets without varying the starting values, but this made the overall model fit very poor.

As one can see in Table S1.5.3, the CFA model fits the data well both statistically (the smallest p value associated with the χ^2 statistic, 0.59, is much larger than 0.05) and heuristically (e.g., the largest SRMR value across all 9 data sets is 0.070, which is smaller than the recommended cutoff value of 0.08). The solution for each data set turned out to be admissible.

The interpretation of the CFA model was also found to be defensible from the climatological point of view. The (direct) effects of the solar and volcanic forcings were well detected in the simulated Sep-Feb temperatures in Australasia during the period 850–1849 AD (e.g., for data set no. 1, $\widehat{Ssim} = 0.022$ with p value$= 7.5e{-}07$, $\widehat{Vsim} = 0.081$ with p value$= 1.2e{-}33$). The (direct) effect of the orbital forcing was estimated as the most modest among the effects of the purely natural forcings

535 (e.g., for Data set no. 1, $\widehat{Osim} = 0.015$ with p value$= 0.032$).

The (direct) overall effect of the GHG forcing turned out to be significant (e.g., for data set no. 1, $\widehat{Gsim} = 0.035$ with p value$= 4.2e{-}11$). Taking into consideration that ξ_{GHG}^{S} turned out to be only weakly correlated with one of the simulated temperature responses to the natural forcings, namely the volcanic forcing ($\widehat{\phi}_{VG} = -0.16$ with p value$=0.21$), this strong overall effect indicates that the anthropogenic component in ξ_{GHG}^{S} dominates the natural one. The significant effect of anthropogenic changes in GHG forcing can be justified by an effect in the last about one century of data in the analysed period.

Table S1.5.3. The result of estimating the modified version of the CFA(7, 6) model fitted to the Australasia data.

• *The result for data set no. 1*

Parameter	Estimate	p value	Parameter	Estimate	p value	Parameter	Estimate	p value
$Ssim$	0.022	$7.5e{-}07$	$\sigma^2_{\tilde{\eta}_{\text{internal pseudo}}}$	0.0051	$3.8e{-}10$	$\sigma_{\tilde{\delta}_{\text{GHG}}\,\tilde{\delta}_{\text{comb}}}$	-0.001	0.012
$Osim$	0.015	0.032	$\sigma_{\tilde{\delta}_{\text{Land (anthr)}}\,\tilde{\delta}_{\text{comb}}}$	0.001	$4.4e{-}03$	$\sigma_{\tilde{\delta}_{\text{GHG}}\,\tilde{\eta}_{\text{internal pseudo}}}$	$-3.2e{-}04$	0.57
$Vsim$	0.081	$1.2e{-}33$	$\sigma_{\tilde{\delta}_{\text{Land (anthr)}}\,\tilde{\eta}_{\text{internal pseudo}}}$	0.001	0.06	$\sigma_{\tilde{\delta}_{\text{Orb}}\,\tilde{\delta}_{\text{comb}}}$	0.001	0.023
$Gsim$	0.035	$4.2e{-}11$	$\sigma_{\tilde{\delta}_{\text{Land (anthr)}}\,\tilde{\delta}_{\text{Sol}}}$	$3.7e{-}04$	0.041	$\sigma_{\tilde{\delta}_{\text{Orb}}\,\tilde{\eta}_{\text{internal pseudo}}}$	$3.3e{-}04$	0.33
ϕ_{VG}	-0.16	0.21	$\sigma_{\tilde{\delta}_{\text{Land (anthr)}}\,\tilde{\delta}_{\text{Orb}}}$	$3.6e{-}04$	0.043			

To assess the overall model fit:

Model $\chi^2 = 12.25$, df $= 14$, p value $= 0.59$, GFI $= 0.97$, AGFI $= 0.94$, SRMR $= 0.070$.

• *Summary of the results based on all 9 data sets*

	Min	Mean	Max		Min	Mean	Max		Min	Mean	Max
$\widehat{Ssim}$	0.019	0.021	0.023	$\widehat{\sigma}_{\tilde{\delta}_{\text{Land (anthr)}}\,\tilde{\delta}_{\text{comb}}}$	$5.9e{-}04$	$6.9e{-}04$	$8.3e{-}04$	Model χ^2	4.5	7.3	12.2
$\widehat{Osim}$	0.015	0.016	0.017	$\widehat{\sigma}_{\tilde{\delta}_{\text{Land (anthr)}}\,\tilde{\eta}_{\text{internal pseudo}}}$	$1.2e{-}04$	$6.8e{-}04$	$9.7e{-}04$	p value	0.59	0.90	0.99
$\widehat{Vsim}$	0.080	0.081	0.082	$\widehat{\sigma}_{\tilde{\delta}_{\text{Land (anthr)}}\,\tilde{\delta}_{\text{Orb}}}$	$3.5e{-}04$	$3.6e{-}04$	$3.6e{-}04$	GFI	0.97	0.98	0.99
$\widehat{Gsim}$	0.034	0.036	0.037	$\widehat{\sigma}_{\tilde{\delta}_{\text{Land (anthr)}}\,\tilde{\delta}_{\text{Sol}}}$	$3.6e{-}04$	$3.9e{-}04$	$4.2e{-}05$	AGFI	0.94	0.96	0.98
$\widehat{\phi}_{VG}$	-0.25	-0.19	-0.14	$\widehat{\sigma}^2_{\tilde{\eta}_{\text{internal pseudo}}}$	0.0035	0.0041	0.0051	SRMR	0.050	0.059	0.070
$\widehat{\sigma}_{\tilde{\delta}_{\text{GHG}}\,\tilde{\delta}_{\text{comb}}}$	-0.0012	-0.001	-0.001	$\widehat{\sigma}_{\tilde{\delta}_{\text{Orb}}\,\tilde{\delta}_{\text{comb}}}$	$2.9e{-}04$	$4.1e{-}04$	$5.7e{-}04$				
$\widehat{\sigma}_{\tilde{\delta}_{\text{GHG}}\,\tilde{\eta}_{\text{internal pseudo}}}$	$3.0e{-}04$	$4.1e{-}04$	$5.7e{-}04$	$\widehat{\sigma}_{\tilde{\delta}_{\text{Orb}}\,\tilde{\eta}_{\text{internal pseudo}}}$	$-1.4e{-}04$	$4.1e{-}04$	$8.8e{-}04$				

The solution for each data set is admissible.

540

The path diagram of the resulting SEM model is shown in Fig. S1.5.1. This SEM model demonstrated the best fit to the data and the most stable performance among different versions of the basic SEM model considered. According to Table S1.5.4, the SEM model fits the data well both statistically (the smallest p value associated with the χ^2 statistic, 0.58, is much larger than 0.05) and heuristically (e.g., the largest SRMR value across all 9 data sets is 0.076, which is smaller than the recommended cutoff value of 0.08). The solution for each data set turned out to be admissible.
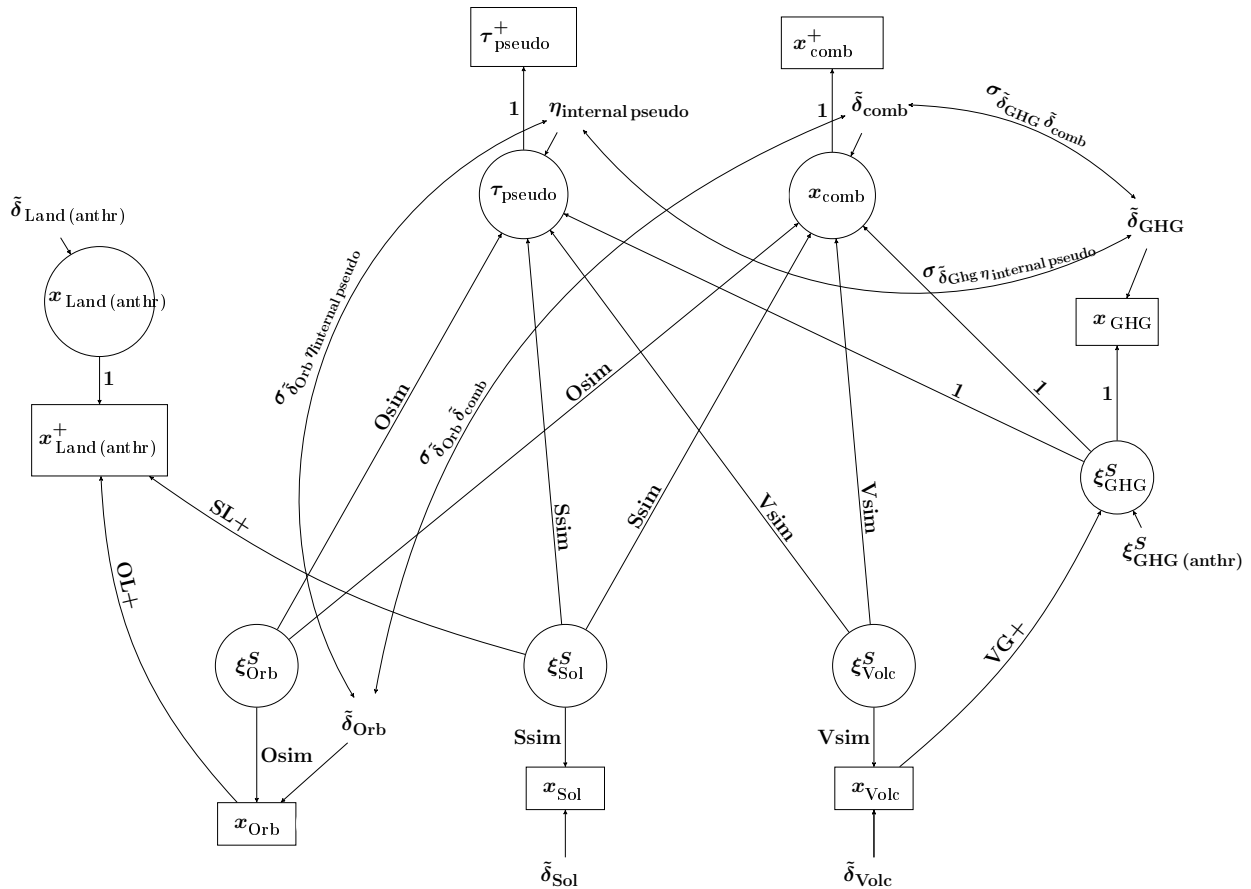
Figure S1.5.1. Path diagram of the SEM model fitted to the Australasia data.

As one can see in Fig. S1.5.1, the SEM model, just as the CFA model above, does not contain the forced component $\xi^S_{\text{Land (anthr)}}$, which corresponds to hypothesising that the direct effect of the land-use forcing is not detectable. However, in contrast to the CFA model, the SEM model contains a new observable variable $x^+_{\text{Land (anthr)}}$, which represents a copy of $x_{\text{Land (anthr)}}$.

550 The variable was constructed in an analogous way and for the same reason as $x^+_{\text{Land (anthr)}}$ in the SEM model fitted to the Europe data (see Sect. S1.1 here). In the absence of $\xi^S_{\text{Land (anthr)}}$, both $x^+_{\text{Land (anthr)}}$ and $x_{\text{Land (anthr)}}$, treated now as a latent variable, represent only the internal temperature variability, denoted $\tilde{\delta}_{\text{Land (anthr)}}$.

As follows from Fig. S1.5.1, $x^+_{\text{Land (anthr)}}$ is "influenced" by ξ^S_{Sol} and x_{Orb} (see the paths $SL+$ and $OL+$, respectively). In the real-world climate system, such causal co-relations between the forced and internal temperature variability could be explained 555 by various interactions (feedback mechanisms) between the internal processes and the climate system.

Table S1.5.4. The result of estimating the SEM model depicted in Fig. S1.5.1 (region: Australasia).

• *The result for data set no. 1*

Parameter	Estimate	p value	Parameter	Estimate	p value	Parameter	Estimate	p value
$Ssim$	0.022	1.4e–07	$VG+$	-0.06	0.18	$\sigma_{\tilde{\delta}_{\text{GHG}}\,\tilde{\eta}_{\text{internal pseudo}}}$	-0.0003	0.59
$Osim$	0.015	0.041	$SL+$	0.017	0.015	$\sigma_{\tilde{\delta}_{\text{Orb}}\,\tilde{\delta}_{\text{comb}}}$	0.001	0.015
$Vsim$	0.081	9.8e–34	$OL+$	0.243	0.054	$\sigma_{\tilde{\delta}_{\text{Orb}}\,\tilde{\eta}_{\text{internal pseudo}}}$	0.0004	0.28
$\text{Var}(\xi^S_{\text{GHG (anthr)}})$	0.001	0.002	$\sigma_{\tilde{\delta}_{\text{GHG}}\,\tilde{\delta}_{\text{comb}}}$	-0.001	0.014	$\sigma^2_{\eta_{\text{internal pseudo}}}$	0.0051	3.8e–10

$$\sqrt{\widehat{\text{Var}}(\xi^S_{\text{GHG}})} = \widehat{Gsim}_{SEM} = \sqrt{(\widehat{VG+})^2 \cdot (\widehat{Vsim}^2 + \sigma^{2*}_{\tilde{\delta}_{\text{Volc}}}) + \widehat{\text{Var}}(\xi^S_{\text{GHG (anthr)}})} = 0.033 \quad (p\text{ value} = 0.001)$$

To assess the overall model fit:

$$\text{Model } \chi^2 = 14.21, \quad \text{df} = 16, \quad p\text{ value} = 0.58, \quad \text{GFI} = 0.96, \quad \text{AGFI} = 0.93, \quad \text{SRMR} = 0.076.$$

• *Summary of the results based on all 9 data sets*

	Min	Mean	Max		Min	Mean	Max		Min	Mean	Max
$\widehat{Ssim}$	0.020	0.022	0.023	$\widehat{VG+}$	-0.081	-0.067	-0.058	Model χ^2	6.3	9.7	14.2
$\widehat{Osim}$	0.014	0.015	0.016	$\widehat{SL+}$	0.016	0.017	0.017	p value	0.58	0.86	0.98
$\widehat{Vsim}$	0.080	0.081	0.081	$\widehat{OL+}$	0.241	0.243	0.245	GFI	0.96	0.97	0.98
$\widehat{\text{Var}}(\xi^S_{\text{GHG (anthr)}})$	0.001	0.001	0.001	$\widehat{\sigma}_{\tilde{\delta}_{\text{Orb}}\,\tilde{\delta}_{\text{comb}}}$	3.2e–04	4.4e–04	6.0e–04	AGFI	0.93	0.95	0.97
$\widehat{\sigma}_{\tilde{\delta}_{\text{GHG}}\,\tilde{\delta}_{\text{comb}}}$	-0.0012	-0.001	-0.001	$\widehat{\sigma}_{\tilde{\delta}_{\text{Orb}}\,\eta_{\text{internal pseudo}}}$	3.6e–04	3.9e–04	4.2e–05	SRMR	0.059	0.065	0.076
$\widehat{\sigma}_{\tilde{\delta}_{\text{GHG}}\,\tilde{\eta}_{\text{internal pseudo}}}$	-0015	-0.001	-0.0003	$\widehat{\sigma}^2_{\eta_{\text{internal pseudo}}}$	0.0035	0.0041	0.0051				
$\widehat{Gsim}$	0.032	0.034	0.035								

The solution for each data set is admissible.

Another model variable, which receives causal inputs, is ξ^S_{GHG}. According to Fig. S1.5.1, ξ^S_{GHG} receives causal inputs from 560 x_{Volc} (see the path $VG+$) and $\xi^S_{\text{GHG (anthr)}}$. In the real-world climate system, the co-relation, given by the path $VG+$, could be explained by interactions between the concentrations of greenhouse gases in the atmosphere and the climate system. Therefore, we may say that just as the CFA model above, the SEM model suggests that ξ^S_{GHG} contains both anthropogenic and natural components. Moreover, just as the CFA model, the SEM model suggests that the anthropogenic component dominates the

34

natural one. This is reflected by the fact that the estimate of $\mathrm{Var}\xi^S_{\mathrm{GHG\,(anthr)}}$ turned out to be significant (across all data sets), while the estimate of *VG+* was insignificant. Finally, the SEM model also estimates the overall effect of the GHGs forcing, given by the parameter *Gsim$_{SEM}$*, as significant across all data sets (e.g. for data set no. 1, $\widehat{Gsim}_{SEM}$=0.033 with p value=0.001).

The direct effects of the solar and volcanic forcings are also estimated as highly significant (e.g., for data set no. 1, $\widehat{Ssim} = 0.022$ with p value$= 1.4e{-}07$, $\widehat{Vsim} = 0.081$ with p value$= 9.8e{-}34$). In contrast, the effect of the orbital forcing was found to be weakly pronounced in the simulated Sep-Feb temperatures in Australasia during the period $850-1849$ AD (e.g., for data set no. 1, $\widehat{Ssim} = 0.015$ with p value$= 0.041$).

S1.5.5   Summary and conclusions (region: Australasia)

The first statistical model, the ME-CFA(6, 5) model, demonstrated a poor performance, which was reflected by inadmissble solutions or the nonconvergence of the estimation procedure.

In contrast, both CFA and SEM models demonstrated an acceptable performance and a very good (almost similar) overall fit to the data. The solutions provided by both statistical models were admissible. Importantly, both models led to similar conclusions about the direct effects of the forcings considered. The estimated direct effects seems to be climatologically defensible for the region and period of interest. Given the similar results provided by both models results and the fact that the SEM model requires additional calculations afterwards, our suggestion is to choose the CFA model as a final model in accordance with the principle of parsimony.

S1.6 Antarctica (annual mean temperature)

The data analysed are presented in Table S1.6.1, from which it follows that six data sets were analysed. Results for the CFA and SEM models are provided in Tables S1.6.2 and S1.6.3, respectively.

Table S1.6.1. Overview of the replicates of each x_{f}, used to construct six regional Antarctica data sets. Each data set contains different $\bar{x}_{\mathrm{comb}}$ and τ_{pseudo}, where $\bar{x}_{\mathrm{comb}}$ is constructed by averaging over three replicates randomly selected from the five that remained after $x_{\mathrm{comb\,repl.}i}$:s, $i = 1, 5, 6, 7$, have been eliminated and after one of $x_{\mathrm{comb\,repl.}i}$:s, $i = 2, 3, 4, 8, 9, 10$, is chosen to represent τ, i.e. τ_{pseudo}.

		Mean sequences			
Data set	$x_{\mathrm{Sol}},\ x_{\mathrm{Volc}}, x_{\mathrm{Land\,(anthr)}},$	x_{Orb}	x_{GHG}	x_{comb}	$x_{\mathrm{comb\,repl.}i} = \tau_{\mathrm{pseudo}}$
1	all associated repl's	1,2		$3, 8, 10$	2
2	all associated repl's	1,2		$4, 9, 10$	3
3	all associated repl's	1,2		$2, 3, 9$	4
4	all associated repl's	1,2		$2, 3, 4$	8
5	all associated repl's	1,2		$2, 4, 10$	9
6	all associated repl's	1,2		$2, 4, 8$	10

580 ### S1.6.1 Preliminary analyses of the single-forcing ensembles by means of the CFA($k_{\mathbf{f}}, 1$) model

As a beginning, let us point out that the independently estimated specific factor variance $\sigma^{2*}_{\tilde{\delta}_{\mathrm{GHG}}}$ turned out to be larger than the sample variance of the mean x_{GHG}-sequence. The interpretation of this result is that the effect of the GHG forcing is not detected in the simulated annual mean Antarctica temperature generated by the x_{GHG}-climate model. This conclusion was supported by the CFA($k_{\mathrm{GHG}} = 2, 0$) model, fitted to the x_{GHG} ensemble and demonstrated a good fit to the data both statistically
585 or heuristically. Another forcings whose effects were assessed as negligible by the CFA($k_{\mathrm{f}}, 0$) model were the orbital and land use forcings, respectively.

Hence, we may say that the preliminary analysis of the single-forcing ensembles indicated that x_{GHG}, x_{Orb} and $x_{\mathrm{Land\,(anthr)}}$ may contain only the internal random temperature variability, represented by the specific factors $\tilde{\delta}_{\mathrm{GHG}}$, $\tilde{\delta}_{\mathrm{Orb}}$ and $\tilde{\delta}_{\mathrm{Land\,(anthr)}}$, respectively.

590 In contrast, it was found that the effects of the solar and volcanic forcings may be well pronounced in the annual mean Antarctica temperature generated by the corresponding single-forcing climate models. The associated estimates of α_{f}, $\mathrm{f} \in$ {Sol, Volc}, provided by CFA($k_{\mathrm{f}}, 1$) model, turned out to be: $\widehat{\alpha}_{\mathrm{Sol}} = 0.058$ with p value$= 3.0e{-}08$, $\widehat{\alpha}_{\mathrm{Volc}} = -0.091 with p value$= 5.1e{-}19$.

S1.6.2 The result of fitting the ME-CFA(6, 5) model to the Antarctica data

595   The result fo estimating the ME-CFA(6, 5) model is that the estimation procedure failed to converge to a solution for each data set. Given the preliminary knowledge that the effect of the three forcings may be negligible, it was expected to observe some consequences of the empirical underidentifiability.

S1.6.3 The result of fitting the CFA(6, 5) model to the Antarctica data

In order to avoid inadmissible solutions and to increase the number of degrees of freedom, the CFA(7, 6) model was estimated

600   under the restrictions that *Lsim*, *Gsim*, *Osim*, and all correlation coefficients, associated with ξ^S_{GHG}, ξ^S_{Orb} and $\xi^S_{\text{Land (anthr)}}$, are zero. In the case of the Antarctica data, the increase in the degrees of freedom was especially desired. This is because it turned out that too many observed variables, including those hypothesised to contain only the internal temperature variability, exhibit very strong correlations with each other. In order to explain such a complex variance-covariance structure, it was necessary to free up a large number of parameters. As one can see in Table S1.6.2, the resulting CFA model estimates 18 parameters, which

605   is the largest number of parameters observed for a CFA model so far. As a consequence, the resulting model has the lowest number of degrees of freedom among all CFA models presented.

    A positive consequence of freeing up so many parameters is that an acceptable model fit both in terms of the χ^2 statistics and the heuristic goodness-of-fit indices could be achieved. The CFA model also demonstrated a stable performance across all data sets. Nevertheless, as pointed out above, freeing up so many parameters led to a substantial loss of degrees of freedom.

610   Probably, this could be avoided if the correlatedness between the specific factors was statistically modelled by means of regressions instead of covariances. Let us investigate this possibility by applying the SEM model specification.

S1.6.4 The result of fitting the SEM model to the Antarctica data

The movement from the CFA specification to the SEM specification was based on the suggestions provided by the modification indices. According to them, significant improvements of the overall model fit could be achived if $x_{\text{Land (anthr)}}$, x_{Orb} and x_{GHG} get

615   various causal inputs from other model variables.

    To be able to do it without changing the interpretation of these three variables from the climate modelling perspective, three new variables were constructed. The variables are: $x^+_{\text{Land (anthr)}}$, x^+_{Orb} and x^+_{GHG}. They were constructed in the same way as $x^+_{\text{Land (anthr)}}$ in the SEM model applied to the Europe data (see the details in Sect. S1.1 here). According to Fig. S1.6.1, two of the three variables, namely $x^+_{\text{Land (anthr)}}$ and x^+_{Orb}, receive causal inputs from x_{comb}, τ_{pseudo} and x_{Sol}. The third one, x^+_{GHG}, gets a

620   causal input from $x^+_{\text{Land (anthr)}}$, which actually means that x^+_{GHG} gets indirect inputs from x_{comb}, τ_{pseudo} and x_{Sol} via $x^+_{\text{Land (anthr)}}$. Thus, the SEM model suggests that the internal climate variability, generated by the $x_{\text{Land (anthr)}}$, x_{Orb}, and x_{GHG} climate models, is related to the temperature variability forced by the reconstructions of the solar and volcanic forcings, as well as to the internal temperature variability generated by the x_{Sol}, and multi-forcing climate models.

    In the real-world climate system, the presence of such co-relations between true temperature responses could be explained

625   by feedback mechanisms between the internal processes and the climate system. Although no dynamical relationships between

Table S1.6.2. The result of estimating the modified version of CFA(7, 6) model fitted to the Antarctica data.

- *The result for data set no. 1*

Parameter	Estimate	p value	Parameter	Estimate	p value	Parameter	Estimate	p value
$Ssim$	0.060	$2.4e{-}17$	$\sigma_{\tilde\delta_{\text{Orb}}\,\tilde\delta_{\text{Land (anthr)}}}$	0.002	0.045	$\sigma_{\tilde\delta_{\text{Land (anthr)}}\,\tilde\delta_{\text{comb}}}$	0.0013	0.13
$Vsim$	0.091	$3.9e{-}32$	$\sigma_{\tilde\delta_{\text{Volc}}\,\tilde\delta_{\text{Land (anthr)}}}$	0.002	0.044	$\sigma_{\tilde\delta_{\text{Land (anthr)}}\,\eta_{\text{internal pseudo}}}$	0.005	$3.2e{-}04$
$\sigma^2_{\eta_{\text{internal pseudo}}}$	0.015	$8.8e{-}09$	$\sigma_{\tilde\delta_{\text{GHG}}\,\tilde\delta_{\text{Land (anthr)}}}$	0.002	$6.4e{-}03$	$\sigma_{\tilde\delta_{\text{GHG}}\,\tilde\delta_{\text{comb}}}$	0.002	0.17
$\sigma_{\tilde\delta_{\text{Sol}}\,\tilde\delta_{\text{Orb}}}$	0.003	$5.7e{-}03$	$\sigma_{\tilde\delta_{\text{Sol}}\,\tilde\delta_{\text{GHG}}}$	0.002	0.070	$\sigma_{\tilde\delta_{\text{GHG}}\,\eta_{\text{internal pseudo}}}$	0.003	0.033
$\sigma_{\tilde\delta_{\text{Sol}}\,\tilde\delta_{\text{Volc}}}$	0.004	$3.0e{-}05$	$\sigma_{\tilde\delta_{\text{Orb}}\,\tilde\delta_{\text{GHG}}}$	0.002	0.13			
$\sigma_{\tilde\delta_{\text{Orb}}\,\tilde\delta_{\text{Volc}}}$	0.002	0.10	$\sigma_{\tilde\delta_{\text{Orb}}\,\tilde\delta_{\text{comb}}}$	0.005	$1.3e{-}04$			
$\sigma_{\tilde\delta_{\text{Sol}}\,\tilde\delta_{\text{Land (anthr)}}}$	0.003	$6.1e{-}04$	$\sigma_{\tilde\delta_{\text{Orb}}\,\eta_{\text{internal pseudo}}}$	0.004	0.013			

To assess the overall model fit:

$$\text{Model } \chi^2 = 7.64, \quad \text{df} = 10, \quad p \text{ value} = 0.66, \quad \text{GFI} = 0.98, \quad \text{AGFI} = 0.94, \quad \text{SRMR} = 0.075.$$

- *Summary of the results based on all 6 data sets*

	Min	Mean	Max		Min	Mean	Max		Min	Mean	Max
$\widehat{Ssim}$	0.060	0.062	0.064	$\widehat\sigma_{\tilde\delta_{\text{GHG}}\,\tilde\delta_{\text{Land (anthr)}}}$	0.0023	0.0023	0.0023	Model χ^2	5.7	8.1	10.1
$\widehat{Vsim}$	0.094	0.096	0.100	$\widehat\sigma_{\tilde\delta_{\text{Sol}}\,\tilde\delta_{\text{GHG}}}$	0.0015	0.0016	0.0018	p value	0.43	0.62	0.84
$\widehat\sigma^2_{\eta_{\text{internal pseudo}}}$	0.0153	0.0206	0.0239	$\widehat\sigma_{\tilde\delta_{\text{Orb}}\,\tilde\delta_{\text{GHG}}}$	0.0016	0.0017	0.0017	GFI	0.97	0.98	0.98
$\widehat\sigma_{\tilde\delta_{\text{Sol}}\,\tilde\delta_{\text{Orb}}}$	0.0025	0.0026	0.0028	$\widehat\sigma_{\tilde\delta_{\text{Orb}}\,\tilde\delta_{\text{comb}}}$	0.0037	0.0048	0.0056	AGFI	0.92	0.94	0.96
$\widehat\sigma_{\tilde\delta_{\text{Sol}}\,\tilde\delta_{\text{Volc}}}$	0.0037	0.0040	0.0042	$\widehat\sigma_{\tilde\delta_{\text{Orb}}\,\eta_{\text{internal pseudo}}}$	0.0006	0.0045	0.0062	SRMR	0.069	0.076	0.086
$\widehat\sigma_{\tilde\delta_{\text{Orb}}\,\tilde\delta_{\text{Volc}}}$	0.0018	0.0020	0.0023	$\widehat\sigma_{\tilde\delta_{\text{Land (anthr)}}\,\tilde\delta_{\text{comb}}}$	0.0031	0.0039	0.0044				
$\widehat\sigma_{\tilde\delta_{\text{Sol}}\,\tilde\delta_{\text{Land (anthr)}}}$	0.0024	0.0025	0.0025	$\widehat\sigma_{\tilde\delta_{\text{Land (anthr)}}\,\eta_{\text{internal pseudo}}}$	0.0025	0.0037	0.0050				
$\widehat\sigma_{\tilde\delta_{\text{Orb}}\,\tilde\delta_{\text{Land (anthr)}}}$	0.0017	0.0018	0.0018	$\widehat\sigma_{\tilde\delta_{\text{GHG}}\,\tilde\delta_{\text{comb}}}$	0.0010	0.0020	0.0027				
$\widehat\sigma_{\tilde\delta_{\text{Volc}}\,\tilde\delta_{\text{Land (anthr)}}}$	0.0018	0.0019	0.0200	$\widehat\sigma_{\tilde\delta_{\text{GHG}}\,\eta_{\text{internal pseudo}}}$	0.0000	0.0018	0.0032				

The solution for each data set is admissible.

the forcing reconstructions and the internal processes were implemented in the climate modelling experiment under consideration, observing such co-relations in the simulated climate system, in our opinion, characterises the climate model (with the forcing reconstructions implemented and its theoretical physical basis) as a realistic representation of the real-world climate system.

630   According to the numerical results given in Table S1.6.3, the estimates of some causal inputs are insignificant or weakly significant (e.g., for data set no. 1, $\widehat{TO+}$=0.029 with p value of 0.70, $\widehat{SO+} = 0.228$ with p value of 0.06, and $\widehat{CL+} = 0.032$ with p value of 0.67). The estimates of the remaining causal inputs are significant (e.g., for data set no. 1, $\widehat{CO+} = 0.208$ with p value= 0.023, $\widehat{TL+} = 0.139$ with p value= 0.026, $\widehat{SL+}$=0.273 with p value= $5.9e{-}03$, and $\widehat{LG+} = 0.299$ with p value= $6.5e{-}$ 03). However, the SEM model (as well as all other models presented so far) still reflects the basic assumption of our framework
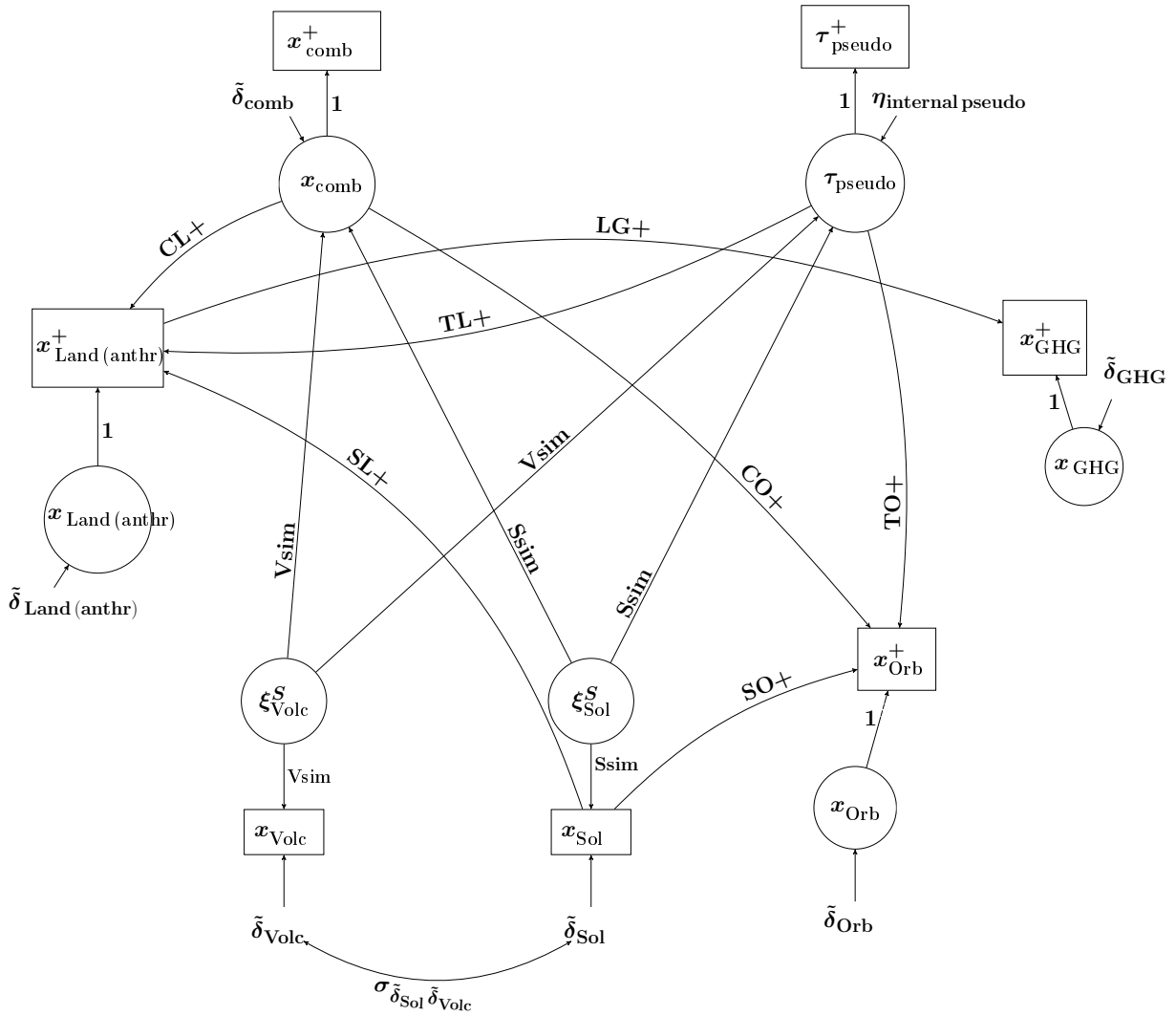
Figure S1.6.1. Path diagram of the SEM model fitted to the Antarctica data.

that the internal processes do not have a systematic effect (of any significance) on the climate. This is follows from the fact that neither $x^+_{\text{Land (anthr)}}$, x^+_{Orb} or x^+_{GHG} affect x_{comb} or τ_{pseudo}.

In contrast, the SEM model detects a significant effect of the solar respectively volcanic forcing in the simulated annual mean temperature in Antarctica during $850-1849$ AD (e.g. for data set no. 1, $\widehat{Ssim} = 0.062$ with p value$= 2.1e\text{–}17$, $\widehat{Vsim} = 0.100$ with p value$= 3.8e\text{–}32$). Once again, the estimated effect of the volcanic forcing turned out to be the strongest.

Table S1.6.3. The result of estimating the SEM model depicted in Fig. S1.6.1 (region: Antarctica).

- *The result for data set no. 1*

Parameter	Estimate	p value	Parameter	Estimate	p value
$Ssim$	0.062	$2.1e{-}17$	$TO+$	0.029	0.70
$Vsim$	0.100	$3.8e{-}32$	$SO+$	0.228	0.06
$\sigma^2_{\eta_{\text{internal pseudo}}}$	0.015	$9.4e{-}09$	$CL+$	0.032	0.67
$\sigma_{\tilde{\delta}_{\text{Sol}}\,\tilde{\delta}_{\text{Volc}}}$	0.0044	$3.2e{-}05$	$TL+$	0.139	0.026
$CO+$	0.208	0.023	$SL+$	0.273	$5.9e{-}03$
			$LG+$	0.299	$6.5e{-}03$

To assess the overall model fit:

Model $\chi^2 = 13.14$,   df $= 17$, p value $= 0.73$,   GFI $= 0.96$,   AGFI $= 0.94$,   SRMR $= 0.071$.

- *Summary of the results based on all 6 data sets*

	Min	Mean	Max		Min	Mean	Max		Min	Mean	Max
$Ssim$	0.062	0.064	0.065	$TO+$	-0.147	0.037	0.136	Model χ^2	9.5	12.7	16.6
$Vsim$	0.095	0.097	0.100	$SO+$	0.207	0.232	0.267	p value	0.48	0.74	0.92
$\sigma^2_{\eta_{\text{internal pseudo}}}$	0.015	0.021	0.024	$CL+$	0.032	0.150	0.227	GFI	0.95	0.96	0.97
$\sigma_{\tilde{\delta}_{\text{Sol}}\,\tilde{\delta}_{\text{Volc}}}$	0.0039	0.0041	0.0043	$TL+$	-0.034	0.039	0.139	AGFI	0.92	0.94	0.96
$CO+$	0.070	0.190	0.340	$SL+$	0.229	0.251	0.273	SRMR	0.061	0.070	0.078
				$LG+$	0.299	0.299	0.299				

The solution for each data set is admissible.

Concerning the overall fit of the SEM model, the numerical results in Table S1.6.3 indicate that the SEM model fits the data well both statistically and heuristically. The p values, associated with the χ^2 statistic, are high across all data sets, and the heuristic measures (GFI, AGFI and SRMR) satisfy the associated cutoff criteria.

S1.6.5   Summary and conclusions (region: Antarctica)

The first statistical model, the ME-CFA(6, 5) model, could not be estimated because the estimation procedure did not converge to a solution.

Both CFA and SEM models have admissible solutions and an acceptable overall fit to the data. Moreover, each statistical model demonstrated a stable performance across the data sets. Importantly, both models led to the same conclusions about the direct effects of forcings, namely that the effects of the volcanic and solar forcings are well detected in the simulated annual mean temperature in Antarctica during 850–1849 AD, while the effects of the land-use, orbital and GHG forcings are not detected. This interpretation seems to be climatologically defensible for the region and period under study. Moreover, this interpretation is supported by the preliminary analyses of the single-forcing ensembles by means of the CFA(k_{f}, 1) model,

which increases our confidence in the conclusions drawn. Thus, we may say that both CFA and SEM models could be chosen as a tentative model of the underlying structure of the data.

However, the SEM model has a great advantage, namely that the SEM model estimates seven parameters less than the CFA
655   model. This is the largest difference between the degrees of freedom observed for the CFA and SEM models fitted to one and the same regional data. Note that this is despite the fact that the variance-covariance structure of the Antarctica data turned out to be more complex than those associated with other regions (which was reflected by a larger number of very significant observed covariances). All these together speak in favor of the SEM model. Therefore, our suggestion is to choose the SEM model, depicted in Fig. S1.6.1, as a statistically adequate and climatologically defensible approximation of the underlying
660   relationships for the simulated annual mean temperature data from Antarctica, covering the period of the 850−1849 AD.

S2 Definition and basic concepts of Structural Equation Model (SEM)

S2.1 A general definition of SEM

The general full SEM model is represented by three equations (Jöreskog and Sörbom, 1988):

$$\text{Latent variable model:} \qquad \boldsymbol{\eta} = \boldsymbol{B}\boldsymbol{\eta} + \boldsymbol{\Gamma}\boldsymbol{\xi} + \boldsymbol{\zeta} \tag{S1}$$

665

$$\text{Measurement model for } \boldsymbol{y}: \quad \boldsymbol{y} = \boldsymbol{\Lambda}_y\boldsymbol{\eta} + \boldsymbol{\epsilon} \tag{S2}$$

$$\text{Measurement model for } \boldsymbol{x}: \quad \boldsymbol{x} = \boldsymbol{\Lambda}_x\boldsymbol{\xi} + \boldsymbol{\delta} \tag{S3}$$

where

$\boldsymbol{\eta}$ an $m \times 1$ vector of latent endogenous variables;

670

$\boldsymbol{\xi}$ an $n \times 1$ vector of latent exogenous variables;

$\boldsymbol{\zeta}$ an $m \times 1$ vector of latent (random) errors in equations;

$\boldsymbol{B}$ an $m \times m$ matrix of coefficients, representing direct effects of η variables on other η variables. $\boldsymbol{B}$ always has zeros in the diagonal, which ensures that a variable is not an immediate cause of itself;

$\boldsymbol{\Gamma}$ an $m \times n$ matrix of coefficients, representing direct effects of ξ variables on η variables;

$\boldsymbol{y}$ a $p \times 1$ vector of observed indicators of $\boldsymbol{\eta}$;

$\boldsymbol{x}$ a $q \times 1$ vector of observed indicators of $\boldsymbol{\xi}$;

$\boldsymbol{\epsilon}$ a $p \times 1$ vector of measurement errors for $\boldsymbol{y}$;

$\boldsymbol{\delta}$ a $q \times 1$ vector of measurement errors for $\boldsymbol{x}$;

$\boldsymbol{\Lambda}_y$ a $p \times m$ matrix of coefficients relating $\boldsymbol{y}$ to $\boldsymbol{\eta}$;

$\boldsymbol{\Lambda}_x$ a $q \times n$ matrix of coefficients relating $\boldsymbol{x}$ to $\boldsymbol{\xi}$.

Within the present work, the normality of data is assumed. Further, it is also assumed that

- $\text{E}(\boldsymbol{\eta}) = 0$, $\text{E}(\boldsymbol{\xi}) = 0$, $\text{E}(\boldsymbol{\zeta}) = 0$, $\text{E}(\boldsymbol{\epsilon}) = 0$, and $\text{E}(\boldsymbol{\delta}) = 0$,

675
- $\boldsymbol{\zeta}$ is uncorrelated with $\boldsymbol{\xi}$ (otherwise, inconsistent coefficient estimators are likely),

- $\boldsymbol{\epsilon}$ is uncorrelated with $\boldsymbol{\eta}$, $\boldsymbol{\xi}$, and $\boldsymbol{\delta}$

- $\boldsymbol{\delta}$ is uncorrelated with $\boldsymbol{\xi}$, $\boldsymbol{\eta}$, and $\boldsymbol{\epsilon}$.

- $\boldsymbol{I} - \boldsymbol{B}$ is nonsingular,

- ζ_{it}, $i = 1, 2, \ldots, m$, is homoscedastic and nonautocorrelated, meaning that the associated covariance matrix of $\boldsymbol{\zeta}$, $\boldsymbol{\Psi}$, is the

680   same for all time points t, and that all observations on ζ_i are mutually uncorrelated. The variance-covariance matrix of $\boldsymbol{\xi}$ is a $n \times n$ symmetrical matrix denoted $\boldsymbol{\Phi}$. That is, exogenous latent variables can be correlated, implying that $\boldsymbol{\Phi}$ is not necessarily diagonal.

According to Bollen (1989, Ch.1), the fundamental hypothesis of structural equation modelling is that the population co-variance matrix of the observed variables, $\mathbf{\Sigma}$, can be written as a function of model parameters, i.e.

$$\mathbf{\Sigma} = \mathbf{\Sigma}(\boldsymbol{\theta}), \tag{S4}$$

685

where $\boldsymbol{\theta}$ denotes a vector of model parameters and $\mathbf{\Sigma}(\boldsymbol{\theta})$ is the model's reproduced (or implied) variance-covariance matrix written as a function of $\boldsymbol{\theta}$, namely

$$\mathbf{\Sigma}(\boldsymbol{\theta}) = \begin{bmatrix} \mathbf{\Sigma}_{yy}(\boldsymbol{\theta}) & \\ \mathbf{\Sigma}_{xy}(\boldsymbol{\theta}) & \mathbf{\Sigma}_{xx}(\boldsymbol{\theta}) \end{bmatrix}, \tag{S5}$$

where

$$\mathbf{\Sigma}_{yy}(\boldsymbol{\theta}) = \mathbf{\Lambda}_y \, \boldsymbol{A} \, (\boldsymbol{\Gamma} \, \boldsymbol{\Phi} \, \boldsymbol{\Gamma}' + \boldsymbol{\Psi}) \, \boldsymbol{A}' \mathbf{\Lambda}_y' + \boldsymbol{\Theta}_\epsilon$$

690

$$\mathbf{\Sigma}_{xy}(\boldsymbol{\theta}) = \mathbf{\Lambda}_x \, \boldsymbol{\Phi} \, \boldsymbol{\Gamma}' \, \boldsymbol{A}' \, \mathbf{\Lambda}_y'$$

$$\mathbf{\Sigma}_{xx}(\boldsymbol{\theta}) = \mathbf{\Lambda}_x \, \boldsymbol{\Phi} \, \mathbf{\Lambda}_x' + \boldsymbol{\Theta}_\delta,$$

where $\boldsymbol{A} = (\boldsymbol{I} - \boldsymbol{B})^{-1}$.

To calculate the variance-covariance matrix of $\boldsymbol{\eta}$, we rewrite Eq. (S1) in the reduced form

$$\boldsymbol{\eta} = (\boldsymbol{I} - \boldsymbol{B})^{-1} \, (\boldsymbol{\Gamma} \, \boldsymbol{\xi} + \boldsymbol{\zeta}). \tag{S6}$$

695

Taking the variance of both sides of Eq. (S6), we obtain

$$\mathbf{\Sigma}_{\boldsymbol{\eta}}(\boldsymbol{\theta}) = (\boldsymbol{I} - \boldsymbol{B})^{-1} \, (\boldsymbol{\Gamma} \, \boldsymbol{\Phi} \, \boldsymbol{\Gamma}' + \boldsymbol{\Psi}) \, \left[(\boldsymbol{I} - \boldsymbol{B})^{-1} \right]'. \tag{S7}$$

An important point to realise about the full SEM is that it subsumes many models as special cases, namely the Measurement Error (ME) model, used in many Detection and Attribution studies, and the Confirmatory Factor Analysis (CFA) model, which
700 we suggested in our analysis.

S2.2   An alternative representation of SEM

The representation of a general structural equation model above is known as a standard representation. Being sufficient for capturing the relation between variables within some analyses, the standard representation might be insufficient within other analyses due to its restrictions. For example, it is not allowed that observed variables influence latent variables, in particular
705 the endogenous ones, which in the context of the present work would prevent climatologically defensible causal links from observable temperatures (simulated and/or observed) to the latent temperature responses due to the land-use and GHG forcings. To overcome those restrictions, one can use the following two-equation model (Bollen, 1989, Ch.9):

$$\boldsymbol{\eta}^+ = \boldsymbol{B}^+ \, \boldsymbol{\eta}^+ + \boldsymbol{\zeta}^+ \tag{S8}$$

$$\boldsymbol{y}^+ = \mathbf{\Lambda}_y^+ \, \boldsymbol{\eta}^+, \tag{S9}$$

710 where $\boldsymbol{\eta}^+$, $\boldsymbol{B}^+$, $\boldsymbol{\zeta}^+$, and $\boldsymbol{y}^+$ are related to the variables from the standard representation in the following way:

$$\boldsymbol{\eta}^+ = \begin{bmatrix} \boldsymbol{y} \\ \boldsymbol{x} \\ \boldsymbol{\eta} \\ \boldsymbol{\xi} \end{bmatrix}, \quad \boldsymbol{\zeta}^+ = \begin{bmatrix} \boldsymbol{\epsilon} \\ \boldsymbol{\delta} \\ \boldsymbol{\zeta} \\ \boldsymbol{\xi} \end{bmatrix}, \quad \boldsymbol{y}^+ = \begin{bmatrix} \boldsymbol{y} \\ \boldsymbol{x} \end{bmatrix}, \quad \boldsymbol{B}^+ = \begin{bmatrix} \boldsymbol{0} & \boldsymbol{0} & \boldsymbol{\Lambda}_y & \boldsymbol{0} \\ \boldsymbol{0} & \boldsymbol{0} & \boldsymbol{0} & \boldsymbol{\Lambda}_x \\ \boldsymbol{0} & \boldsymbol{0} & \boldsymbol{B} & \boldsymbol{\Gamma} \\ \boldsymbol{0} & \boldsymbol{0} & \boldsymbol{0} & \boldsymbol{0} \end{bmatrix}, \quad \boldsymbol{\Lambda}_y^+ = \begin{bmatrix} \boldsymbol{I}_{p+q} & \boldsymbol{0} \end{bmatrix}, \tag{S10}$$

where $\boldsymbol{I}_{p+q}$ is an order-$(p+q)$ identity matrix picking out the observed variables from $\boldsymbol{\eta}^+$. The $\boldsymbol{\Lambda}_y^+$ is consequently $(p+q) \times (p+q+m+n)$. Further,

- $\boldsymbol{\eta}^+$ and $\boldsymbol{\zeta}^+$ are $(p+q+m+n) \times 1$,
- $\boldsymbol{y}^+$ is $(p+q) \times 1$, and
- $\boldsymbol{B}^+$ is $(p+q+m+n) \times (p+q+m+n)$.

The final matrix for this alternative representation is the covariance matrix for $\boldsymbol{\zeta}^+$ denoted $\boldsymbol{\Psi}^+$. Its relation to the standard parameters is

$$\boldsymbol{\Psi}^+ = \begin{bmatrix} \boldsymbol{\Theta}_\epsilon & & & \\ \boldsymbol{0} & \boldsymbol{\Theta}_\delta & & \\ \boldsymbol{0} & \boldsymbol{0} & \boldsymbol{\Psi} & \\ \boldsymbol{0} & \boldsymbol{0} & \boldsymbol{0} & \boldsymbol{\Phi} \end{bmatrix}. \tag{S11}$$

Using the reduced form of $\boldsymbol{\eta}^+$, given by

$$\boldsymbol{\eta}^+ = \left(\boldsymbol{I} - \boldsymbol{B}^+\right)^{-1} \boldsymbol{\zeta}^+, \tag{S12}$$

the reproduced covariance matrix of $\boldsymbol{\eta}^+$ is derived:

$$\boldsymbol{\Sigma}_{\boldsymbol{\eta}^+}(\boldsymbol{\theta}) = \left(\boldsymbol{I} - \boldsymbol{B}^+\right)^{-1} \boldsymbol{\Psi}^+ \left((\boldsymbol{I} - \boldsymbol{B}^+)^{-1}\right)'. \tag{S13}$$

Inserting (S12) into (S9) gives the reproduced covariance matrix of the observed variables only:

$$\boldsymbol{\Sigma}_{\boldsymbol{y}^+}(\boldsymbol{\theta}) = \left(\boldsymbol{\Lambda}_y^+ \left(\boldsymbol{I} - \boldsymbol{B}^+\right)^{-1}\right) \boldsymbol{\Psi}^+ \left(\boldsymbol{\Lambda}_y^+ \left(\boldsymbol{I} - \boldsymbol{B}^+\right)^{-1}\right)' \tag{S14}$$

The matrices $\boldsymbol{B}^+$ from (S10) and $\boldsymbol{\Psi}^+$ from (S11) make explicit the implicit constraints of the standard representation. However, by changing the fixed zero elements in these matrices we can relax many of those constraints. An important point to keep in mind, when relaxing the assumptions of the standard representation, is that the resulting model should be identified.

S2.3 Estimation of parameters of a SEM model

Let us start by describing a classification of parameters, suggested by Jöreskog (1969):

- A *free* parameter is a parameter to be estimated. Since free parameters are not associated with anything specific about them, they are not a part of the hypotheses associated with a factor model.

- A *fixed* parameter is a parameter whose value is prespecified by hypothesis and this value remains unchanged during the iterative estimation process.

44

– A *constrained-equal* parameter is a parameter that is estimated but its value is constrained to be equal to another parameter (or parameters). Because only one value needs to be determined for each group of constrained-equal parameters, only one parameter from this group is counted when counting the number of distinct estimated parameters. In contrast to free parameters, constrained-equal parameters are a part of the hypotheses associated with a factor model, although both types of the parameters are estimated.

Free and constrained-equal parameters are estimated such that the discrepancy between the sample variance-covariance matrix of the indicators, S, and the estimated model's reproduced variance-covariance matrix, $\Sigma(\widehat{\theta})$, is as small as possible. In particular, under the assumption of normality of the data, the estimates are obtained by minimising the following discrepancy function with respect to the free parameters, i.e. the parameters to be estimated, conditional on the explicitly constrained parameters (Jöreskog, 1969; Bollen, 1989; Mulaik, 2010):

$$F(\boldsymbol{\theta}) = \log|\boldsymbol{\Sigma}(\boldsymbol{\theta})| + \mathrm{tr}(\boldsymbol{S}\boldsymbol{\Sigma}(\boldsymbol{\theta})^{-1}) - \log|\boldsymbol{S}| - q', \tag{S15}$$

where $q' = p+q$ is the total number of indicators. In fact, minimising (S15) is equivalent to maximising the maximum likelihood (ML) function (Jöreskog, 1969), meaning that the resulting estimates $\widehat{\boldsymbol{\theta}}$ are ML estimates.

According to the general theory, the ML estimates are consistent, jointly asymptotically normally distributed with the asymptotic variance expressed as being the inverse of the Fisher information. In confirmatory factor analysis, the Fisher information in a matrix form is defined as follows :

$$\frac{n-1}{2} \cdot E\left[\frac{\partial^2 F(\boldsymbol{\theta})}{\partial \boldsymbol{\theta} \partial \boldsymbol{\theta}'}\right]. \tag{S16}$$

The inverse of (S16), evaluated at the values for the parameters that minimise the F function, gives an estimate of the variance of the asymptotic distribution of the model estimates.

One can use the estimated variances to test each estimated parameter θ_i by means of the z statistic $\widehat{\theta_i}\big/\sqrt{\widehat{\mathrm{Var}(\widehat{\theta_i})}}$, which has approximately a standard normal distribution. The results of tests that $\theta_i = 0$ are provided in form of two-sided p values by all statistical packages designed to do SEM, regardless of whether a model is just-identified or overidentified. In addition, one also can construct the approximate $100(1-p)\%$ Wald confidence interval for each parameter θ_i to test $H_0 : \theta_i = \theta_i^0$:

$$\widehat{\theta}_{\mathrm{i}} \pm z_{p/2} \cdot \sqrt{\widehat{\mathrm{Var}(\widehat{\theta}_{\mathrm{f}})}}, \tag{S17}$$

where $z_{p/2}$ is the $100(1-p/2)$ percentile of the standard normal distribution.

S2.4 Assessing the overall SEM model fit to the data and its acceptability

The overall model fit can be assessed statistically by the χ^2 test, and heuristically using a number of goodness-of-fit indices. Closely related to the F function above, the χ^2 test statistic is the log-likelihood ratio test statistic, given by:

$$\chi^2 = -2 \cdot (\log L(H_0) - \log L(H_A)) = (n-1) \cdot F(\widehat{\boldsymbol{\theta}}), \tag{S18}$$

765   where $\log L(H_0) = -\frac{1}{2} \cdot (n-1) \cdot \left\{ \log|\boldsymbol{\Sigma}(\boldsymbol{\theta})| + \mathrm{tr}(\boldsymbol{S}\boldsymbol{\Sigma}(\boldsymbol{\theta})^{-1}) \right\}$ is the logarithm of the likelihood function under the null hypothesis $H_0 : \boldsymbol{\Sigma} = \boldsymbol{\Sigma}(\boldsymbol{\theta})$, while $\log L(H_A) = -\frac{1}{2} \cdot (n-1) \cdot \left\{ \log|\boldsymbol{S}| + q' \right\}$ is the logarithm of the likelihood function under the alternative hypothesis H_A of unrestricted $\boldsymbol{\Sigma}$, i.e. $\boldsymbol{\Sigma} = \boldsymbol{S}$.

In large samples, the χ^2 test statistic is approximately distributed as chi-square with

$$df = q'(q'+1)/2 - m',$$

770   degrees of freedom, where $q'(q'+1)/2$ is the number of the unique (nonduplicated) equations in the variance-covariance matrix of the indicators, and m' is the number of distinct free parameters, i.e. parameters to be estimated. All statistical packages developed for estimating structural equation models, for example $LISREL$, AMOS, the R package sem, provide the observed value of the model χ^2 with the associated p value. The conventional guidelines for interpreting p values are roughly as follows (Cox and Donnelly, 2011):

775   – if $p \approx 0.1$ there is a *suggestion* of evidence against H_0;

– if $p \approx 0.05$ there is modest evidence against H_0;

– if $p \approx 0.01$ there is strong evidence against H_0.

As for goodness-of-fit indices, we use here the following ones: *a goodness-of-fit index* (GFI), GFI adjusted for degrees of freedom (AGFI), and standardised root- mean-square residual (SRMR). Just as with the χ^2 test statistic, the observed values of these

780   three heuristic measures are reported by most statistical sofware programs aiming at estimating structural equation models. The GFI is obtained using the following formula (Sharma, 1996):

$$\mathrm{GFI} = 1 - \frac{\mathrm{tr}(\widehat{\boldsymbol{\Sigma}}^{-1}\boldsymbol{S} - \boldsymbol{I})^2}{\mathrm{tr}(\widehat{\boldsymbol{\Sigma}}^{-1}\boldsymbol{S})^2}, \tag{S19}$$

and represents the amount of variances and covariances in $\boldsymbol{S}$ that are predicted by the SEM model. In this sense it is analogous in interpretation to R^2 in multiple regression. The AGFI is essentially GFI that has been adjusted for degrees of freedom. AGFI

785   is given as (Sharma, 1996)

$$\mathrm{AGFI} = 1 - \frac{q'(q'+1)}{2\,df}(1 - \mathrm{GFI}), \tag{S20}$$

where df are the degrees of freedom, and $q' = p+q$ is the number of indicators. Regarding the cutoff values of these two indices, the following rules of thumb are recommended. The GFI for good-fitting models should be greater than 0.90, while for the AGFI the suggested cutoff value is 0.8 (Sharma, 1996). In contrast to the GFI and AGFI, the SRMR is rather a "badness-of-fit

790   index" than a "goodness-of-fit index". It also ranges between 0 and 1, but 0 indicates perfect fit, while larger values indicate lack of fit. The SRMR is defined as follows (Hu and Bentler, 1999):

$$\mathrm{SRMR} = \sqrt{\frac{\sum_{i=1}^{q'}\sum_{j=1}^{i}\left[(s_{ij} - \widehat{\sigma}_{ij})\big/(s_{ii}s_{jj})\right]^2}{q'(q'+1)/2}}, \tag{S21}$$

where $s_{ij} :=$ observed (co-)variances, $\widehat{\sigma}_{ij} :=$ reproduced (co-)variances, s_{ii} and $s_{jj} :=$ observed standard deviations. According to Hu and Bentler (1999), a cutoff value close to 0.08 for SRMR indicates a good fit. It is worth pointing out that it is recommended to use the goodness-of-fit indices for assessing the fit of a number of competing models fitted to the same data set, rather than the fit of a single model. Researchers also should pay attention to other aspects of model fit such as examining parameter estimates to ensure that they have the anticipated signs and magnitudes. Before considering some type of model modification, other reasons why a model may not fit, such as small sample size, nonnormality, or missing data, need to be ruled out first (Boomsma, 2000).

Note that the SRMR provides a summary measure of the *normalised residuals*, defined as a difference between the sample variance-covariance matrix $\boldsymbol{S}$ and the estimated reproduced variance-covariance matrix $\boldsymbol{\Sigma}(\widehat{\boldsymbol{\theta}})$. Normalisation is accomplished by dividing the residuals by their respective asymptotic standard errors. If a SEM model is rejected, the question then becomes: How can the SEM model be modified to fit the data? Examining the normalised residuals can provide hints or clues to what changes can be made. Large residuals indicate that the hypothesised SEM model is not able to adequately explain the (co-)variances of the indicators. Normalised residuals that exceed 1.96 or 2.58 in absolute value are considered statistically significant at the significance level of 5% and 1%, respectively. Ideally, no more than 5% of normalised residuals should be greater than 1.96. Similarly, no more than 1% should be greater than 2.58.

Another useful tool in the process of model modification is the modification indices. Developed by Sörbom (1989), these indices attempt to estimate which missing paths, if added to the current SEM model, would result in the greatest reduction of the discrepancy between model and data. The way to use these indices is to free the fixed parameter associated with the largest reduction and reanalyse the resulting model.

It should be realised that a good overall model fit alone is not sufficient to accept a SEM model as an appropriate approximation of underlying relationships. To be able to do it, one needs to check whether the solution is admissible and defensible from the climatological point of view. For SEM models standardising only latent (exogenous) variables to have unit variances, inadmissible solutions are indicated by estimated correlations between latent variables that lie outside their admissible range between -1 and 1. If estimated correlations have admissible values a next step is to look at a completely standardised solution. The completely standardised solution is the solution obtained when the variances of both latent variables *and* indicators are one.

If completely standardised estimates of factor loadings exceed 1 in absolut value then the solution obtained is inadmissible. Completely standardised solutions are provided by all statistical software designed to performed SEM analysis, in particular by the R package `sem` employed in the present analysis. Note that the `sem` package requires latent factor variances of 1 to be represented explicitly.

To conclude, only if a SEM model has an acceptable overall fit, assessed both statistically and heuristically, and its solution is admissible and climatologically interpretable then we may accept the SEM model as an approximation of underlying relationships.

S2.5 Assessing the significance of estimated variances of latent endogenous variables

Having estimated the variance of a latent endogenous variable in accordance with Eq. (S7) or Eq. (S13), it is of interest to assess its significance. To this end, one can use the multivariate delta method (Bollen (1989), p.390, and references therein). To apply this method, let us first reiterate that $\widehat{\boldsymbol{\theta}}$ are ML estimates, meaning that they are asymptotically jointly normally distributed with a mean of $\boldsymbol{\theta}$ and a covariance matrix $\mathrm{COV}(\widehat{\boldsymbol{\theta}})$ containing the variances of the estimates down its main diagonal and the covariances off the diagonal. Further, let $f(\widehat{\boldsymbol{\theta}})$ be a function which is differentiable at $\widehat{\boldsymbol{\theta}} = \boldsymbol{\theta}$ so that it can be expanded in a first-order Taylor series about $\boldsymbol{\theta}$. Under these conditions the multivariate delta method states that the asymptotic distribution of $f(\widehat{\boldsymbol{\theta}})$ is normal with a mean of $f(\boldsymbol{\theta})$ and the variance given by

$$\mathrm{Var}(f(\widehat{\theta}_1,\widehat{\theta}_2,\ldots,\widehat{\theta}_{m'})) = \sum_{i=1}^{m'} \mathrm{Var}(\widehat{\theta}_i) \cdot (f_i'(\boldsymbol{\theta}))^2 + 2 \cdot \sum_{i=1}^{m'} \sum_{j=i+1}^{m'} \mathrm{Cov}(\widehat{\theta}_i,\widehat{\theta}_j) \cdot f_i'(\boldsymbol{\theta}) \cdot f_j'(\boldsymbol{\theta}) \tag{S22}$$

where $f_i'(\boldsymbol{\theta})$ denotes the first partial derivative of $f(\widehat{\boldsymbol{\theta}})$ with respect to $\widehat{\theta}_i$, evaluated at $\boldsymbol{\theta} = (\theta_1,\theta_2,\ldots,\theta_{m'})$. For large samples, substituting the sample estimates into (S22) provides an estimate of the variance of the asymptotic distribution of $f(\widehat{\boldsymbol{\theta}})$:

$$\widehat{\mathrm{Var}}(f(\widehat{\theta}_1,\widehat{\theta}_2,\ldots,\widehat{\theta}_{m'})) = \sum_{i=1}^{m'} \widehat{\mathrm{Var}}(\widehat{\theta}_i) \cdot (f_i'(\widehat{\boldsymbol{\theta}}))^2 + 2 \cdot \sum_{i=1}^{m'} \sum_{j=i+1}^{m'} \widehat{\mathrm{Cov}}(\widehat{\theta}_i,\widehat{\theta}_j) \cdot f_i'(\widehat{\boldsymbol{\theta}}) \cdot f_j'(\widehat{\boldsymbol{\theta}}). \tag{S23}$$

Since for large samples

$$\frac{f(\widehat{\boldsymbol{\theta}}) - f(\boldsymbol{\theta})}{\sqrt{\widehat{\mathrm{Var}}(f(\widehat{\boldsymbol{\theta}}))}} \overset{\mathrm{approx}}{\sim} \mathrm{N}(0,1), \tag{S24}$$

we can construct an approximate $100(1-p)\%$ confidence interval for $f(\widehat{\boldsymbol{\theta}})$ as follows:

$$f(\widehat{\boldsymbol{\theta}}) \pm z_{p/2} \cdot \sqrt{\widehat{\mathrm{Var}}(f(\widehat{\boldsymbol{\theta}}))}, \tag{S25}$$

where $z_{p/2}$ is the $100(1-p/2)$ percentile of the standard normal distribution.

Note that $f(\widehat{\boldsymbol{\theta}})$ can be any function of parameter estimates, not necessarily representing the variance of latent exogenous variables. Regardless of the function, it is important that if all the parameters involved are essentially zero, then the delta method cannot be applied to obtain the approximation for the standard error of the estimate of the endogenous parameter of interest.

S3 *R*- and *Matlab*-codes

In the present work we employed the *R* package `sem` (Fox et al., 2014) using *R* version 3.0.2 (R Core Team, 2013) for estimation
850 of all statistical models under study. For derivation of symbolic expressions of the reproduced variance-covariance matrices
associated with our statistical models under different hypotheses, we used Matlab (R2018b (9.5.0.944444) 64-bit (glnxa64)),
in particular its Symbolic Math Toolbox, which provides functions for solving and manupulating symbolic math equations (see
https://se.mathworks.com/help/symbolic/index.html?s_tid=CRUX_lftnav).

S3.1 An example of using the *R* package `sem`

855 Here we exemplify the usage of the *R* package `sem` by providing the code for estimating all three statistical models fitted to
the Europe data: the ME-CFA(6, 5) model, the CFA(7, 6) model and the SEM model. Regardless of the statistical model fitted,
the estimation procedure in the `sem` package involves four steps:

1. Specify the model of interest;

2. Save the specify model into an ASCII file;

860 3. Prepare the data for the analysis, and finally

4. Perform the estimation.

An additional step may be required when analysing SEM models, namely the calculation of the variances of endogenous
variables (if the SEM model of interest contains such variables). Within the context of this work, it is of interest to calculate
the variance of ξ_{GHG}^{S}, provided it receives causal inputs from other model variables.

865 ### S3.1.1 Fitting the ME-CFA(6, 5) model presented in Table S1.1.2 to the Europe data

Step 1. Specify the model (here, in the path format).

```
# Define the factor loadings
xi_Sol -> x_Sol,       Ssim,  NA     # NA denotes an arbitrary starting value for the parameter Ssim
xi_Sol -> tau_pseudo,  Strue, NA
xi_Orb -> x_Orb,       Osim,  NA
xi_Orb -> tau_pseudo,  Otrue, NA
xi_Volc -> x_Volc,     Vsim,  NA
xi_Volc -> tau_pseudo, Vtrue, NA
xi_Land -> x_Land,     Lsim,  NA     #For the sake of simplicity, xi_Land in the R scripts presented
                                     # denotes xi_Land_anthr, while x_Land denotes x_Land_anthr
xi_Land -> tau_pseudo, Ltrue, NA
xi_Ghg -> x_Ghg,       Gsim,  NA
xi_Ghg -> tau_pseudo,  Gtrue, NA
# Define the correlation coefficients
xi_Sol <-> xi_Orb,       phiSO, NA
```

49

```
      xi_Sol <-> xi_Volc,       phiSV, NA
      xi_Sol <-> xi_Land,       phiSL, NA
      xi_Sol <-> xi_Ghg,        phiSG, NA
      xi_Orb <-> xi_Volc,       phiOV, NA
885   xi_Orb <-> xi_Land,       phiOL, NA
      xi_Orb <-> xi_Ghg,        phiOG, NA
      xi_Volc <-> xi_Land,      phiVL, NA
      xi_Volc <-> xi_Ghg,       phiVG, NA
      xi_Land <-> xi_Ghg,       phiLG, NA
890   # Fix the variances of the latent factors to 1 by writing NA in the place of a parameter symbol
      xi_Sol <-> xi_Sol,        NA, 1
      xi_Ghg <-> xi_Ghg,        NA, 1
      xi_Orb <-> xi_Orb,        NA, 1
      xi_Land <-> xi_Land,      NA, 1
895   xi_Volc <-> xi_Volc,      NA, 1
      # Set the variances of the specific factors to the values obtained a priori
      # by means of estimator (2.3) define in LAS22num
      x_Sol <-> x_Sol,          NA,  0.0084   # corresponds to Var(\tilde{\delta}_Sol),
      x_Orb <-> x_Orb,          NA,  0.012    # corresponds to Var(\tilde{\delta}_Orb),
900   x_Volc <-> x_Volc,        NA,  0.00574  # and so on
      x_Land <-> x_Land,        NA,  0.0086
      x_Ghg <-> x_Ghg,          NA,  0.0076
      tau_pseudo <-> tau_pseudo,  NA,  0.02571
```

Step 2. Save the above code into an ASCII file, e.g. *ME_CFA_model_EUR.r*

905 **Step 3.** Prepare the data for the analysis:

```
      # Construct a data set of observed variables, where only tau_pseudo is a single sequence,
      # while the others are mean-sequences
      MYDATA_ME<-cbind(x_Sol, x_Orb, x_Volc, x_Land, x_Ghg, tau_pseudo)
      # Name the observed variables in MYDATA_ME in the same way as in Step 1
910   colnames(MYDATA_ME)<-c("x_Sol","x_Orb", "x_Volc","x_Land","x_Ghg", "tau_pseudo")
      #Compute the variance-covariance matrix of the observed variables
      S2<-cov(MYDATA_ME);
```

Step 4. Estimation

```
      # Load the sem package
915   library(sem)
      # Define the heuristic indices of interest
      opt <- options(fit.indices = c("GFI", "AGFI","SRMR"))
      # Read in the ASCII file with the ME-CFA(6, 5) model
      model_1_EUR<-specifyModel("ME_CFA_model_EUR.r")
```

```
920   # Fit the model and save the results to a model fit object
      result_model_1_EUR<- sem(model_1_EUR, S2,N=100,fit.indices=TRUE) # where N is
                                                                # a number of observations
      # To see the result of the estimation
      summary(result_model_1_EUR)
```

925 **S3.1.2   Fitting the CFA(7, 6) model presented in Table S1.1.3 to the Europe data**

Step 1. Specify the CFA model

```
      # Define the factor loadings
      xi_Sol -> x_Sol,        Ssim, 0.063665
      xi_Sol -> x_comb,       Ssim, 0.063665
930   xi_Sol -> tau_pseudo,    Ssim, 0.063665
      xi_Orb -> x_Orb,         NA, 0
      xi_Orb -> x_comb,        NA, 0
      xi_Orb -> tau_pseudo,    NA, 0
      xi_Volc -> x_Volc,       Vsim, 0.134
935   xi_Volc -> x_comb,       Vsim, 0.134
      xi_Volc -> tau_pseudo,   Vsim, 0.134
      xi_Land -> x_Land,       NA, 0
      xi_Land -> x_comb,       NA, 0
      xi_Land -> tau_pseudo,   NA, 0
940   xi_Ghg -> x_Ghg,         Gsim, 0.0524
      xi_Ghg -> x_comb,        Gsim, 0.0524
      xi_Ghg -> tau_pseudo,    Gsim, 0.0524
      # Set the variance of latent factors to 1
      xi_Sol <-> xi_Sol,       NA, 1
945   xi_Orb <-> xi_Orb,       NA, 1
      xi_Volc <-> xi_Volc,     NA, 1
      xi_Land <-> xi_Land,     NA, 1
      xi_Ghg  <-> xi_Ghg,      NA, 1
      # Define the variance of \eta_internal_pseudo
950   tau_pseudo <-> tau_pseudo,   Var_eta_internal, 0.01917
      # Define the unknown specific factor covariances
      x_Sol <-> x_Ghg,       cov_xSol_xGhg, 0.0025
      x_Land <-> x_Orb,      cov_xLand_xOrb, 0.00020
      x_Land <-> x_Volc,     cov_xLand_xVolc, 0.00126
955   x_Land <-> x_comb,      cov_xLand_xComb, 0.00312
      x_Land <-> tau_pseudo,  cov_xLand_tauPseudo, 0.00312
      ##  Set the variances of the specific factors to the a apriori obtained values
      x_Sol <-> x_Sol,          NA,  0.0084
      x_Orb <-> x_Orb,          NA,  0.012
960   x_Volc <-> x_Volc,        NA,  0.00574
```

```
x_Land <-> x_Land,         NA,  0.0086
x_Ghg <-> x_Ghg,           NA,  0.0076
x_comb <-> x_comb,         NA,  0.00868
```

Step 2. Save the above code into an ASCII file, e.g. *CFA_model_EUR.r*

965 **Step 3.** Prepare the data for the analysis:

```
# Construct a data set of observed variables, where only tau_pseudo is a single sequence,
# while the others are mean-sequences
MYDATA_CFA<-cbind(x_Sol, x_Orb, x_Volc,x_Land, x_Ghg, x_comb, tau_pseudo)
# Name the observed variables in MYDATA_CFA in the same way as in Step 1
970 colnames(MYDATA_CFA)<-c("x_Sol","x_Orb", "x_Volc","x_Land","x_Ghg", "x_comb","tau_pseudo")
#Compute the variance-covariance matrix of the observed variables
S2<-cov(MYDATA_CFA);
```

Step 4. Estimation

```
# Load the sem package
975 library(sem)
# Define the heuristic indices of interest
opt <- options(fit.indices = c("GFI", "AGFI","SRMR"))
# Read in the ASCII file with the CFA(7, 6) model
model_2_EUR<-specifyModel("CFA_model_EUR.r")
980 # Fit the model and save the results to a model fit object
result_model_2_EUR<- sem(model_2_EUR, S2, N=100, fit.indices=TRUE)
# To see the result of the estimation
summary(result_model_2_EUR)
```

S3.1.3 Fitting the SEM model presented in Fig. S1.1.1 to the Europe data

985 **Step 1.** Specify the SEM model

```
eta_Sol -> x_Sol,          Ssim,  0.063665
eta_Sol -> x_comb,         Ssim,  0.063665
eta_Sol -> tau_pseudo,     Ssim,  0.063665
x_Orb  -> x_Orb+,          NA, 1
990 eta_Volc -> x_Volc,        Vsim,  0.13364
eta_Volc -> x_comb,        Vsim,  0.13364
eta_Volc -> tau_pseudo,    Vsim,  0.13364
x_Land  -> x_Land+,        NA, 1          #For the sake of simplicity, x_Land+ in the R scripts presented
                                          # denotes x_Land_anthr+
995 eta_Ghg -> x_Ghg,          NA, 1
eta_Ghg -> x_comb,         NA, 1
```

```
         eta_Ghg -> tau_pseudo,       NA, 1
         x_comb -> x_comb+,           NA, 1
         tau_pseudo -> tau_pseudo+,   NA, 1
1000     ## Introduce the specified causal inputs
         x_Sol       -> eta_Ghg,     SG+, 0.024
         x_comb      -> x_Land+,     CL+, 0.01
         tau_pseudo -> x_Land+,      TL+, 0.01
         x_Land+     -> x_Orb+,      LO+, 0.01
1005     # Define the variance of the disturbance term xi_Ghg_anthr
         xi_Ghg <-> xi_Ghg,        Var_xi_Ghg_anthr, 0.0014
         #  Define the variances of the latent exogenous variables
         xi_Sol <-> xi_Sol,               NA, 1
         xi_Volc <-> xi_Volc,             NA, 1
1010     # Define the variance of \eta_internal_pseudo
         tau_pseudo <-> tau_pseudo,   Var_eta_internal, 0.01621
         # Define the unknown specific-factor covariance
         x_Sol <-> x_Ghg,          cov_xSol_xGhg, 0.00125
         ##  Define the variance of each \delta-term and
1015     ##   set these variances to the a priori obtained values
         x_Sol <-> x_Sol,             NA,  0.0084   # corresponds to Var(\tilde{\delta}_Sol),
         x_Orb <-> x_Orb,             NA,  0.012    # corresponds to Var(\tilde{\delta}_Orb),
         x_Volc <-> x_Volc,           NA,  0.00574  # and so on
         x_Land <-> x_Land,           NA,  0.0086
1020     x_Ghg <-> x_Ghg,             NA,  0.0076
         x_comb <-> x_comb,           NA,  0.00868
         x_Orb+ <-> x_Orb+,           NA, 0         # by definition
         x_Land+ <-> x_Land+,         NA, 0         # by definition
         x_comb+ <-> x_comb+,         NA, 0         # by definition
1025     tau_pseudo+ <->tau_pseudo+,  NA, 0         # by definition
```

Step 2. Save the above code into an ASCII file, e.g. *SEM_model_EUR.r*

Step 3. Prepare the data for the analysis:

```
         # Construct a data set of observed variables, where only tau_pseudo is a single sequence,
         # while the others are mean-sequences
1030     MYDATA_SEM<-cbind(x_Sol, x_Orb, x_Volc,x_Land, x_Ghg, x_comb, tau_pseudo)
         # Name the observed variables in MYDATA_SEM in the same way as in Step 1
         colnames(MYDATA_SEM)<-c("x_Sol","x_Orb+", "x_Volc","x_Land+","x_Ghg","x_comb+", "tau_pseudo+")
         #Compute the variance-covariance matrix of the observed variables
         S2<-cov(MYDATA_SEM);
```

1035 **Step 4.** Estimation

```
         # Load the sem package
```

```
library(sem)
# Define the heuristic indices of interest
opt <- options(fit.indices = c("GFI", "AGFI","SRMR"))
```

1040
```
# Read in the ASCII file with the SEM model
model_3_EUR<-specifyModel("SEM_model_EUR.r")
# Fit the SEM model and save the result to a model fit object
result_model_3_EUR<- sem(model_3_EUR, S2,  N=100,  fit.indices=TRUE)
# To see the result of the estimation
```
1045
```
summary(result_model_3_EUR)
```

```
## Save the parameter estimate as separate objects. They are needed for
## calculating the variance of the endogenous variable $\xi_{\text{Ghg}}\,$ according to
## the delta method described in Sect. S2.5:
```
1050
```
Ssim<-coef(result_model_3_EUR)[[1]]
Vsim<-coef(result_model_3_EUR)[[2]]  # and so on
```

```
## Derive the estimated variance-covariance matrix of the parameter estimates, needed for
## calculating the variance of the endogenous variable $\xi_{\text{Ghg}}\,$ according to
```
1055
```
## the delta method described in Sect. S2.5:
VCOV<-vcov(result_model_3_EUR)
Var_Ssim<- VCOV[1,1]
Var_Vsim<- VCOV[2,2]  # and so on, depending on the order in which the parameters appear
                      # in the summary, i.e. summary(result_model_3_EUR)
```

1060 **S3.2   An example of using Matlab for calculating the variances of latent endogenous variables**

Here we provide the m file used for the calculation of the variance of the latent endogenous variable ξ_{GHG} from the SEM model in Fig. S1.1.1 fitted to the Europe data. The calculations are based on Eq. (S10), Eq. (S11), and Eq. (S13). The variables in these equations, i.e.

$$\eta^+ = \{ y', x', \eta', \xi' \},$$

1065 and

$$\zeta^+ = \{ \epsilon', \delta', \zeta', \xi' \},$$

correspond to the variables of the SEM model under consideration in the following way:

$$y' = \{ x^+_{\text{Land (anthr)}}, x^+_{\text{Orb}}, x_{\text{GHG}}, x^+_{\text{comb}}, \tau^+_{\text{pseudo}} \},$$

1070 $$x' = \{ x_{\text{Sol}}, x_{\text{Volc}} \},$$

$$\boldsymbol{\eta}' = \{x_{\text{Land (anthr)}}, x_{\text{Orb}}, \xi^S_{\text{GHG}}, x_{\text{comb}}, \tau_{\text{pseudo}}\},$$

$$\boldsymbol{\xi}' = \{\xi^S_{\text{Sol}}, \xi^S_{\text{Volc}}\},$$

1075 and

$$\boldsymbol{\epsilon}' = \{0, 0, \delta_{\text{GHG}}, 0, 0\},$$

$$\boldsymbol{\delta}' = \{\delta_{\text{Sol}}, \delta_{\text{Volc}}\},$$

1080 $$\boldsymbol{\zeta}' = \{\tilde{\delta}_{\text{Land (anthr)}}, \tilde{\delta}_{\text{Orb}}, \xi^S_{\text{GHG (anthr)}}, \tilde{\delta}_{\text{comb}}, \eta_{\text{internal pseudo}}\}.$$

```
%% Define the variables in Matlab as follows
    Ssim=sym('Ssim');
    Vsim=sym('Vsim');
1085 CLplus=sym('CLplus');
    TLplus=sym('TLplus');
    LOplus=sym('LOplus');
    xi_Ghg_anthr=sym('xi_Ghg_anthr');
    psi_Ghg=sym('psi_Ghg');   % In order to simplify notation, the parameter psi_Ghg denotes
1090                          %  here the variance of the disturbance term xi^S_Ghg_anthr,
    SGplus=sym('SGplus');
    delta_Sol=sym('delta_Sol');
    delta_Orb=sym('delta_Orb');
    delta_Volc=sym('delta_Volc');
1095 delta_Land=sym('delta_Land');
    delta_Ghg=sym('delta_Ghg');
    delta_comb=sym('delta_comb');
    eta_internal_pseudo=sym('eta_internal_pseudo');
    xi_Sol=sym('xi_Sol');
1100 xi_Volc=sym('xi_Volc');
    var_delta_Sol=sym('var_delta_Sol');
    var_delta_Orb=sym('var_delta_Orb');
    var_delta_Volc=sym('var_delta_Volc');
    var_delta_Land=sym('var_delta_Land');
1105 var_delta_Ghg=sym('var_delta_Ghg');
    var_delta_comb=sym('var_delta_comb');
    var_eta_internal_pseudo=sym('var_eta_internal_pseudo');
    cov_deltaSol_deltaGhg=sym('cov_deltaSol_deltaGhg');
```

%% Define the B^+, I^+ and ζ^+ matrices in accordance with Eq. (S10):

```
1110 B_plus=[     0, 0, 0, 0, 0,     0, 0, 1, 0, 0, CLplus, TLplus,    0,    0;
            LOplus, 0, 0, 0, 0,     0, 0, 0, 1, 0,     0,      0,    0,    0;
```

```
                0, 0, 0, 0, 0,       0, 0, 0, 0, 1,      0,      0,    0,    0;
                0, 0, 0, 0, 0,       0, 0, 0, 0, 0,      1,      0,    0,    0;
                0, 0, 0, 0, 0,       0, 0, 0, 0, 0,      0,      1,    0,    0;
1115            0, 0, 0, 0, 0,       0, 0, 0, 0, 0,      0,      0, Ssim,    0;
                0, 0, 0, 0, 0,       0, 0, 0, 0, 0,      0,      0,    0, Vsim;
                0, 0, 0, 0, 0,       0, 0, 0, 0, 0,      0,      0,    0,    0;
                0, 0, 0, 0, 0,       0, 0, 0, 0, 0,      0,      0,    0,    0;
                0, 0, 0, 0, 0, SGplus, 0, 0, 0, 0,      0,      0,    0,    0;
1120            0, 0, 0, 0, 0,       0, 0, 0, 0, 0,      0,      0, Ssim, Vsim;
                0, 0, 0, 0, 0,       0, 0, 0, 0, 0,      0,      0, Ssim, Vsim;
                0, 0, 0, 0, 0,       0, 0, 0, 0, 0,      0,      0,    0,    0;
                0, 0, 0, 0, 0,       0, 0, 0, 0, 0,      0,      0,    0,    0];


1125 I_plus=eye(14);


     zeta_Plus=[0;
                0;
                delta_Ghg;
1130            0;
                0;
                delta_Sol;
                delta_Volc;
                delta_Land;
1135            delta_Orb;
                xi_Ghg_anthr;
                delta_comb;
                eta_internal_pseudo;
                xi_Sol;
1140            xi_Volc];

     %% Define the $\Psi^+$ matrix in accordance with Eq. (S11):

     Psi_plus=[0, 0, 0, 0, 0, 0,  0, 0, 0, 0, 0, 0, 0, 0;
               0, 0, 0, 0, 0, 0,  0, 0, 0, 0, 0, 0, 0, 0;
               0, 0, var_delta_Ghg,  0, 0, cov_deltaSol_deltaGhg, 0, 0, 0, 0, 0, 0, 0, 0;
1145          0, 0, 0, 0, 0, 0,  0, 0, 0, 0, 0, 0, 0, 0;
               0, 0, 0, 0, 0, 0,  0, 0, 0, 0, 0, 0, 0, 0;
               0, 0, cov_deltaSol_deltaGhg, 0, 0, var_delta_Sol, 0, 0, 0, 0, 0, 0, 0, 0;
               0, 0, 0, 0, 0, 0,var_delta_Volc,  0, 0, 0,  0, 0, 0, 0;
```

```
                   0, 0, 0, 0, 0, 0,  0, var_delta_Land, 0, 0, 0, 0, 0, 0;
1150               0, 0, 0, 0, 0, 0,  0, 0, var_delta_Orb, 0, 0, 0, 0, 0;
                   0, 0, 0, 0, 0, 0,  0, 0, 0, psi_Ghg, 0, 0, 0, 0;
                   0, 0, 0, 0, 0, 0,  0, 0, 0, 0,var_delta_comb, 0, 0, 0;
                   0, 0, 0, 0, 0, 0,  0, 0, 0, 0, 0, var_eta_internal_pseudo, 0, 0;
                   0, 0, 0, 0, 0, 0,  0, 0, 0, 0, 0, 0, 1, 0;
1155               0, 0, 0, 0, 0, 0,  0, 0, 0, 0, 0, 0, 0, 1];
```

%% Define the variance-covariance matrix of η^+ in accordance with Eq.(S13):

```
Var_eta_plus=(inv(I_plus-B_plus))*Psi_plus*transpose(inv(I_plus-B_plus));
```

%% Extract the expression of the variance of the endogenous variable ξ_{GHG}^S from the matrix above:

```
Var_etaGhg=Var_eta_plus(10,10)
```

1160 %%One obtaines the following equation:

```
Var_etaGhg = SGplus^2*Ssim^2 + var_delta_Sol*SGplus^2 + psi_Ghg
```

%% Derive the expressions of the first derivates of $\mathrm{Var}(\xi_{\mathrm{GHG}}^S)$ with respect to the parameters involved:

```
f(SGplus)=var_etaGhg;  Deriv_wrt_SGplus = diff(f,SGplus)
f(psi_Ghg)=var_etaGhg; Deriv_wrt_psiGhg = diff(f,psi_Ghg)
```
1165 ```
f(Ssim)=var_etaGhg;   Deriv_wrt_Ssim = diff(f,Ssim)
```

%%The resulting derivatives are:

```
Deriv_wrt_SGplus(SGplus) = 2*SGplus*Ssim^2 + 2*SGplus*var_delta_Sol
Deriv_wrt_psiGhg(psi_Ghg) = 1
Deriv_wrt_Ssim(Ssim) = 2*SGplus^2*Ssim
```

1170 The resulting symbolic equations are to be used when calculating the variance of the endogenous variable ξ_{GHG}^S in accordance with the delta method described in Sect. S2.5. In the present analysis, the numerical evaluation of the resulting symbolic equations has been performed in R using the estimates obtained in Step 4 of the estimation procedure of the SEM model (see Sect. S3.1.3).

References

1175 Berger, A. L.: Long-term variations of daily insolation and Quaternary climatic changes, J. Atmos. Sci., 35, 2362–2367, https://doi.org/10.1175/1520-0469(1978)035<2362:LTVODI>2.0.CO;2, 1978.

Bollen, K. A.: Structural equations with latent variables, Wiley, 1989.

Boomsma, A.: Reporting Analyses of Covariance Structures, Structural Equation Modeling: A Multidisciplinary Journal, 7, 461-483, https://doi.org/10.1207/S15328007SEM0703_6, 2000.

1180 Cox, D. R., and Donnelly, C. A.: Principles of Applied Statistics, Cambridge university press, 2011.

Crowley, T. J., Zielinski, G., Vinther, B., Udisti R., Kreutz K., Cole-Dai, J., and Castellano, E.: Volcanism and the Little Ice Age, PAGES Newsletter, 16, 22–23, https://doi.org/10.22498/pages.16.2.22, 2008.

Gao, C. C., Robock, A., and Ammann, C.: Volcanic forcing of climate over the past 1500 years: an improved ice core-based index for climate models, J. Geophys. Res., 113, D23111, https://doi.org/10.1029/2008JD010239, 2008.

1185 Fetisova, E., Moberg, A., and Brattström, G.: Towards a flexible statistical modelling by latent factors for evaluation of simulated responses to climate forcings: LAS22num (Supplement), http://su.diva-portal.org/smash/get/diva2:1150165/FULLTEXT02.pdf.

Fox, J., Nie, Z., Byrnes, J., Culbertson, M., DebRoy, S., Friendly, M., Goodrich, B., Jones, R. H., Kramer, A., Monette, G., and R-Core: sem: Structural Equation Models, R package version 3.1-5, http://CRAN.R-project.org/package=sem, 2014.

Hu, L. and Bentler, P.M.: Cutoff criteria for fit indices in covariance structure analysis: Conventional criteria versus new alternatives, Struc-
1190 tural Equation Modeling: A Multidisciplinary Journal, 6, 1-55, https://doi.org/10.1080/10705519909540118, 1999.

Hurtt, G. C., Chini, L. P., Frolking, S., Betts, R., Feddema, J., Fischer, G., Goldewijk, K. K., Hibbard, K., Janetos, A., Jones, C., Kindermann, G., Kinoshita, T., Riahi, K., Shevliakova, E., Smith, S., Stehfest, E., Thomson, A., Thornton, P., van Vuuren, D., Wang, Y.: Harmonization of global land-use scenarios for the period 1500-2100 for IPCC AR5. ILEAPS Newsletter, 7, 6-8, https://scholars.unh.edu/earthsci_facpub/488, 2009.

1195 Jöreskog, K. G.: A general approach to confirmatory maximum likelihood factor analysis. Psychometrika, 34, 183-202, https://doi.org/10.1007/BF02289343, 1969.

Jöreskog, K. G., and Sörbom, D.: LISREL 7: a guide to the program and applications, SPSS INC, 1988.

Landrum, L., Otto-Bliesner, B. L., Wahl, E. R., Conley, A., Lawrence, P.J., Rosenbloom, N., and Teng, H. Last millennium climate and its variability in CCSM4, J. Climate, 26, 1085–1111, https://doi.org/10.1175/JCLI-D-11-00326.1, 2013.

1200 Lashgari, K., Moberg, A., and Brattström, G.: Evaluation of simulated responses to climate forcings: from Detection and Attribution studies to a new flexible statistical framework (numerical experiment), 2022.

Mulaik, S. A.: Linear causal modeling with structural equation, Chapman&Hall/CRC, 2009.

Mulaik, S. A.: Foundations of Factor Analysis, 2nd edition, Chapman&Hall/CRC, 2010.

Otto-Bliesner, B. L., Brady, E. C., Fasullo, J., Jahn, A., Landrum, L., Stevenson, S., Rosenbloom, N., Mai, A. and Strand, G.: Climate
1205 variability and changes since 850 CE: An Ensemble Approach with the Community Earth System Model, Bulletin of the American Meteorological Society, 97, 735-754, https://doi.org/10.1175/BAMS-D-14-00233.1, 2016.

Pongratz, J., Reick, C., Raddatz, T., and Claussen, M.: A reconstruction of global agricultural areas and land cover for the last millennium, Global Biogeochem. Cycles, 22, GB3018, https://doi.org/10.1029/2007GB003153, 2008.

R Core Team: R: A Language and Environment for Statistical Computing, R Foundation for Statistical Computing, Vienna, Austria, http:
1210 //www.R-project.org/, 2013.

Sharma, S.: Applied multivariate techniques, Wiley, 1996.

Schmidt, G. A., Jungclaus, J. H., Ammann, C. M., Bard, E., Braconnot, P., Crowley, T. J., Delaygue, G., Joos, F., Krivova, N. A., Muscheler, R., Otto-Bliesner, B. L., Pongratz, J., Shindell, D. T., Solanki, S. K., Steinhilber, F., and Vieira, L. E. A.: Climate forcing reconstructions for use in PMIP simulations of the last millennium (v1.0), Geosci. Model Dev., 4, 33–45, https://doi.org/10.5194/gmd-4-33-2011, 2011.

1215 Schmidt, G. A., Jungclaus, J. H., Ammann, C. M., Bard, E., Braconnot, P., Crowley, T. J., Delaygue, G., Joos, F., Krivova, N. A., Muscheler, R., Otto-Bliesner, B. L., Pongratz, J., Shindell, D. T., Solanki, S. K., Steinhilber, F., and Vieira, L. E. A.: Climate forcing reconstructions for use in PMIP simulations of the Last Millennium (v1.1), Geosci. Model Dev., 5, 185–191, https://doi.org/10.5194/gmd-5-185-2012, 2012.

Sundberg, R., Moberg, A., and Hind, A.: Statistical framework for evaluation of climate model simulations by use of climate proxy data from 1220 the last millennium- Part 1: Theory, Clim Past, 8, 1399-1353, https://doi.org/10.5194/cp-8-1339-2012, 2012.

Sörbom, D.: Model Modification, Psychometrika, 54, 371-384, https://doi.org/10.1007/BF02294623, 1989.

Vieira, L. E. A., Solanki, S. K., Krivova, N. A., and Usoskin, I.: Evolution of the solar irradiance during the Holocene, Astron. Astroph., 531, A6, https://doi.org/10.1051/0004-6361/201015843, 2011.

Wang, Y.-M., Lean J. L., and Sheeley N. R., Jr.: Modeling the Sun's Magnetic Field and Irradiance since 1713, ApJ, 625, 522–538, 1225 https://doi.org/10.1086/429689, 2005.